Canadian Science Publishing
NRC Research Press journals | Publishing Services

Canadian Geotechnical Journal
Revue canadienne de géotechnique

PILE GROUPS UNDER DEEP EXPANSION. A CASE HISTORY

Journal:	*Canadian Geotechnical Journal*
Manuscript ID:	cgj-2014-0407.R1
Manuscript Type:	Article
Date Submitted by the Author:	n/a
Complete List of Authors:	Alonso, Eduardo; Universidad Politecnica de Cataluna Sauter, Simon; ETH Zurich, Ramon, Anna; Universitat Politècnica de Catalunya,
Keyword:	pile-groups, heave, case history, analytical solutions, anhydritic claystone

Date paper written: September 25, 2014

PILE GROUPS UNDER DEEP EXPANSION. A CASE HISTORY

Eduardo E. Alonso — Professor of Geotechnical Engineering. Department of Geotechnical Engineering and Geosciences. Universitat Politècnica de Catalunya, Barcelona, Spain.

Simon Sauter — Civil Engineer. Department of Geotechnical Engineering and Geosciences. Universitat Politècnica de Catalunya, Barcelona, Spain.

Anna Ramon — Civil Engineer. Department of Geotechnical Engineering and Geosciences. Universitat Politècnica de Catalunya, Barcelona, Spain.

Corresponding author:

Eduardo Alonso
Department of Geotechnical Engineering and Geosciences.
Edificio D-2. Campus Nord. UPC. 08034 Barcelona
Phone: 34 93 401 6862; 34 93 401 7256
Fax: 34 93 401 7251
e-mail: eduardo.alonso@upc.edu

PILE GROUPS UNDER DEEP EXPANSION. A CASE HISTORY

E.E. Alonso, S. Sauter & A. Ramon
Dep. of Geotechnical Engineering & Geosciences, UPC, Barcelona

ABSTRACT:

A viaduct in a high speed railway line experienced severe heave of its central pillars as a result of deep expansion of an anhydrite rock. Bridge pillars were founded on pile groups which experienced vertical heave displacements as well as lateral displacements and rotations. A semi-analytical solution for the response of a pile group under loading and arbitrary located soil expansion was developed integrating fundamental solutions for the elastic half-space. The procedure was first validated and then applied to explain the recorded behaviour of the pile groups. The deep expansion was identified from independent surface heave and continuous extensometer readings. Group rotations were well predicted. Observed tensile fissures at the cap-pile contact were explained by the calculated forces and moments on the piles.

KEYWORDS: pile-groups, heave, case history, analytical solutions, anhydritic claystone.

INTRODUCTION

Soon after construction, a railway bridge, whose pillars were founded on 3 × 3 large diameter (1.65 m) bored piles, experienced a sustained heave of its central spans. The geological profile along the bridge length is shown in Figure 1. Central pillars 5 and 6 are supported by 20 m long piles embedded in a Tertiary clay rock having variable content of gypsum and anhydrite. The upper length of shafts crosses Tertiary brown firm clay. A thin colluvial layer covers the Tertiary substratum.

The measured heave at the level of the bridge deck reached maximum values of 250 mm in the period 2002–2007 (Fig. 2).

Extensometer data revealed the presence of a deep active layer, 10–12 m thick, located under the pile's tip. The geometry of the pile group under pillar 5 and the recorded strains by means of a

sliding micrometer (Kovári & Amstad, 1982) is shown in Figure 3. No deformations are recorded along the length of pile's shaft. However, the micrometer detected an increasing swelling strain at depth, at distances in excess of 3 m from the pile's tip.

The integrity of the piles and the pile-cap contact was investigated by a few borings drilled from the surface of the pile cap. These borings were drilled in piles belonging to the groups supporting pillars 4, 5, 6 and 7. Overall, 12 piles were investigated (3 borings per pillar). All the borings were observed by optical cameras. Tensile fissures were systematically detected at the interface between the pile's heads and the heavily reinforced 3.5 m thick pile cap. This observation was tentatively interpreted as a justification for a swelling process developing on the upper brown clay before the extensometer observations ruled out this possibility.

The scenario revealed by these observations in the sense that some pile groups were subjected to heave developing below the pile tip level, is very singular and no precedents in the geotechnical literature have been found. Piles on expansive soils are typically found on places where a surface active layer of high plasticity clay is subjected to cyclic drying and wetting cycles, and, therefore, to cyclic shrinkage and swelling straining on the upper parts of shafts. Calculation procedures for this loading scenario are available (Nelson & Miller, 1992; Poulos & Davis, 1980).

The case outlined brings interesting issues regarding the behaviour of pile groups under such special type of loading. Obviously the involved groups experienced an overall heave. But lateral displacements, as well as cap rotations were measured. They contributed to straining the bridge pillars and set in danger the integrity of the entire viaduct. In addition the fissures observed at the pile-cap contact revealed significant and unexpected pile loadings which could hardly be explained.

The case has been described in Alonso & Ramon (2013) and Ramon & Alonso (2013), paying attention to the reasons and mechanisms of the deep heave phenomenon. It was concluded that the heave was associated with the presence of anhydrite in the rock formation located under the piles' tip. The expansion of the active layer was explained by the precipitation of gypsum crystals in water saturated rock discontinuities. This expansion is not homogeneous because of the relevant role of

rock fracturing to explain the heave. Therefore, it is expected that the deep heave will be irregular and this irregularity will be determinant to understand the reaction of the pile group.

The basic problem can be stated in the following terms: find the response of a pile group when a unit volumetric expansion takes place at an arbitrary location within the soil. Then, if the distribution of volumetric heave at depth can be estimated, the basic solution may be used to derive the response of the pile group to an arbitrary expansion of the active layer. The basic problem has been solved in semi-analytical terms making use of fundamental solutions for the elastic half space, as described in the next section. This was the first step to analyse the real case described before. Field observations of surface heave provided data to identify the spatial distribution of the volumetric expansion of the active layer.

The model response has been compared with the measured performance of the central pile groups of the bridge. The analysis provided a satisfactory explanation for the field observations as well as a validation for the method of analysis developed.

PROBLEM FORMULATION

Pile groups pose some difficulties for numerical analysis: their geometry requires a 3D discretization, it combines structural elements (piles, cap) and a continuum soil "matrix" and it includes widely different characteristic dimensions (the pile's diameter and the area of influence of the group). This makes it unreasonable in many cases to use available finite element programs to design pile groups.

On the other hand, semi-analytic methods combining closed form fundamental solutions for point loads in elastic half spaces led to powerful solutions, which resulted in easy to use dimensionless graphs (Poulos & Davis, 1980) or to rapid calculation programs, which may handle complex geometries (GEO5 and Pdisp). This simpler approach is favoured in this work because it is believed to provide solutions sufficiently accurate for the purposes of investigating the effect of soil

114 expansion on pile groups specially when dealing with relatively rigid soil or clay rock formations,
115 which is the case described here.

116 The case to be solved is sketched in Figure 4. A group of piles (N_p piles following a given layout in
117 plan view - (x, y) plane -), having a length L and a diameter d is subjected to a system of forces
118 (moment M, vertical load F_v and horizontal load F_h) acting against the pile cap. Distributed normal
119 and shear forces f_v and f_h may act on the soil surface. A volume increase ΔV develops at an arbitrary
120 point (x, y, h) within the soil. The unknowns are the deformations and forces acting on every pile
121 and the overall group deformation. The method of analysis is illustrated in Figure 5 for an ideal
122 case, which is selected to describe the calculation procedure.

123 Let us assume that the group and the soil surface are acted by horizontal loads. In addition, the soil
124 experiences a volume increase at a given point. The problem is solved by making compatible the
125 deformation of two independent "structures": the pile group and the soil. The interaction forces, p_{ij},
126 act on each of these structures. They are the problem unknowns. They may be found by forcing a
127 compatibility of the displacements of the two structures and by ensuring equilibrium of forces. This
128 approach was probably first described, for a single pile, by Jiménez Salas & Belzunce (1965). It
129 was later applied to solve an increasing number of pile and soil conditions. Poulos & Davis (1980)
130 provide a comprehensive account. The equilibrium and displacement compatibility conditions
131 expressed in a few discrete points (or elements in which the piles are discretized) lead to a set of
132 algebraic equations for the interaction forces, which solves the problem (more details of the
133 formulation are given in Appendix 1).

134 Displacements of the half space are calculated by superposition using three fundamental solutions:
135 Boussinesq (1885) for point loading on the surface, Mindlin (1936) for concentrated forces inside
136 the half space and Sagaseta (1987) for the displacements induced by the expansion or contraction of
137 a spherical source.

The outlined formulation is conditioned by additional assumptions, which may be adopted to simplify the analysis. The model adopted relies on the following set of simplifications:

– Heave deformations in points of the half space are calculated by means of the "paved half space" case of the Sagaseta (1987) solution. This implies neglecting the correcting shear forces acting on the surface of the half space. The effect of these forces is small, especially in the case analysed here, because of the depth of the swelling sources.

– Displacements induced by a given swelling volume are solved by means of the superposition of elementary spherical sources.

– The calculation of vertical soil displacements distinguishes two cases: the displacements along the elements of a given pile and the displacements associated with the interaction among piles. In the first case, the shear forces acting on the pile shaft are assumed to be equivalent to a uniform load distributed on the cross-section of the pile. Mindlin (1936) solution for a concentrated load is integrated on this surface. Interaction between piles (always within the "soil structure") is solved by means of the analytical solutions for the concentrated load.

– Horizontal stresses applied by the elements of a pile are assumed to act against a rectangular surface. The width of this surface is calculated by making equal the moment of inertia of the circular section and an equivalent square section.

– The horizontal deformation of a pile subjected to a bending moment and a horizontal force at the pile top, as well as a set of horizontal loads distributed along the pile shaft is solved by integrating the differential equation of elastic equilibrium.

– Soil displacements are calculated at the centre of each pile element. The necessary integration of Mindlin (1936) solution is done numerically.

– When calculating the interaction among piles, the normal or shear stresses at a given pile acting on an element of a neighbouring pile are made equivalent to concentrated loads acting on the centre of the elements that discretize the piles.

– The pile cap is assumed to be rigid. Pile tops remain in a plane. The initial distribution of vertical loads on piles is calculated from the applied external total vertical load and the two bending moments considering the moments of inertia of a given distribution of piles. Horizontal loads on piles are distributed uniformly. Once an initial pile load distribution is determined, vertical displacements are calculated. They are then forced to remain in a plane by adjusting the displacements to the average displacement that is calculated by minimizing the sum of deviation errors. Then, a new set of vertical pile displacements is calculated. The procedure requires an iterative calculation.

The outlined method has been programmed in Matlab. The program requires the following set of data:

– Position, length and diameter of piles in a group.

– Number of discretization elements per pile.

– Soil parameters: elastic modulus and Poisson ratio.

– Position, geometry and intensity of the swelling "bubble".

– Distributed load on the surface of the half space.

– Forces and moments acting on the pile cap.

The program has been named "CANDÍ" after the name of the railway bridge experiencing the foundation problem ("Pont de Candí").

VALIDATION OF THE CALCULATION METHOD

Two benchmark sets of solutions have been selected to validate the CANDÍ program: some cases solved in Poulos & Davis (1980) and specific calculations performed with Plaxis 3D.

Vertical load on a single pile

The comparison of shaft shear stresses is plotted in Figure 6 for the following case: pile length, L = 25 m; pile diameter, d = 1 m; pile elastic modulus, $E_p = 3 \times 10^7$ kPa; soil elastic modulus, $E_s = 10^5$ kPa; soil Poisson's coefficient, ν_s = 0.5; vertical load on pile: 3000 kN. The pile response is calculated for two values of the stiffness factor, $K = E_p\, R_A/E_s$, of the pile (K = 50 and K = 5000), where R_A is the area of the transversal section of the pile divided by the area bounded by the outer circumference of pile. The pile stiffness factor K measures the relative compressibility of the pile and the soil. The higher the relative compressibility of the pile with respect to the soil, the smaller the value of K. Results are almost identical.

Horizontal force and moment on a single pile

The pile is acted either by a horizontal load H = 3000 kN or else by a top moment M = 5000 kN·m. A flexibility factor $K_R = E_p\, I_p / E_s\, L^4$ is defined for the pile and two dimensionless extreme cases (K_R = 1 and $K_R = 10^{-4}$) are selected to compare results. The remaining parameters correspond to the case of a vertical load on a single pile.

The cases selected for comparison are a single pile under horizontal load at the top and free pile head (represented in Figure 7). Lateral earth pressures and bending moments are compared for the two widely different flexibility coefficients. CANDÍ and Poulos & Davis (1980) results are very close. Other cases, not illustrated here, of successful comparison, refer to a single pile under a moment applied at the top and free pile head and a single pile under horizontal top load and clamped head.

Pile group under vertical load

A 3 × 3 pile group, which reproduces the foundation of the central pillars of the Candí viaduct, was selected for the analysis. Pile numbering is given in Figure 8a. A 3D Plaxis model is sketched in Figures 8b and 8c. A large volume (400 × 400 × 300 m) was discretized to avoid any boundary effect. Piles are simulated by means of structural elements available in Plaxis code. The pile cap has a thickness of 3.50 m. The finite element mesh was refined around the piles. The following set of data reproduces approximately the conditions of the pile group under pillar 5 of the viaduct: E_s = 10^5 kPa; $\nu_s = 0.3$; L = 20 m; d = 1.65 m; $E_p = 3 \times 10^7$ kPa; $P_{v\ group}$ = 27000 kN. Figure 9 compares Plaxis 3D and CANDÍ results for the distribution of vertical loads on piles 1, 2 and 5. The agreement is very good.

Pile group under horizontal load

Pile group parameters are maintained but now a horizontal load $P_{h\ group}$ = 27000 kN is applied. Horizontal pile displacements and bending moment distribution along the shaft of Pile 5 are compared in Figures 10a and 10b. The largest difference is calculated for the clamping moment at the top of pile 5 (Fig. 10b), which is smaller in Plaxis. This is probably a result associated with a difference on the top rotation of the two calculations, but overall, the agreement is quite satisfactory.

It was concluded that, despite the simplifications introduced, the program developed could reproduce reasonably well the behaviour of pile groups embedded in an elastic soil. It is a fast running program and it was used to analyse the reaction of the pillar foundations against the deep heave. Before this is done, the swelling intensity and distribution at depth should be characterized in a precise way. A very useful data in this regard was the observed heave at the surface. A large area on both sides of the viaduct was instrumented by surface marks that were regularly levelled. A definite pattern of heave displacements was identified. This information was interpreted with the help of program CANDÍ with the purpose of defining the swelling characteristics at the source. The

three fundamental solutions introduced in the calculation model (Boussinesq 1885, Mindlin 1936 and Sagaseta 1987) refer to a half space bounded by a horizontal surface. This is not exactly the case of the topography in the vicinity of the Pillar 5, which will be analyzed below. However, the area around the pillar (60x60 m) can be approximated by a plane having an inclination of 13º in the transversal direction to the valley, and a slope around 2º-3º in the direction of the valley. This is a reasonably horizontal surface for the purposes of the analysis performed, described in the next section.

INTENSITY AND DISTRIBUTION OF THE SWELLING SOURCE

Extensometers installed in boreholes along the bridge provided information on the position of the active layer (Fig. 11). This is an approximate piece of information because some extensometers do not penetrate the entire active zone. The intensity of swelling is not reflected in Figure 11. This is better appreciated if surface contours of equal heave for a given period are examined (Fig. 12) (5 months in the plot). Also shown in this figure is the position of the viaduct pillars. The iso-displacement curves can be described as irregular ellipses whose main axis follows the direction of the valley crossed by the viaduct. The largest heave is located a few meters upstream of pillar 5. If an axis perpendicular to the valley at the position of pillar 5 is taken as a reference, it can be observed that the distribution of heave is not symmetrical with respect to this axis: heave is more intense in the downstream direction. This feature indicates that the heave phenomenon is also controlled to some extent by the natural flow pattern in the valley.

The challenge now is to approximate the distribution of heave at depth knowing the information provided by extensometers located along the direction of the viaduct and the surface pattern of heave. It was decided to investigate the effect of locating swelling sources at the mid-level of the active layer. Since the active layer extends at depths varying from z = 24 m to z= 34 m below the deepest point in the valley, the sources were located at z = 29 m.

It was also found useful to investigate the effect of different patterns of swelling sources. A number of swelling source distributions, sketched in Figure 13, were analysed. The plots in Figure 13 show the distribution of the swelling intensity, measured in terms of volume. In all cases, a common total swelling volume increment ΔV = 318 m^3 was imposed. This is the heave volume calculated by interpreting the volume under the contour lines given in Figure 12. The first case in Figure 13 represents a continuous line of equal swelling sources. The second and third cases correspond to heterogeneous distribution of sources. The variable $\hat{a}$ or $\tilde{a}$ in Figure 13 provide the relative value of the swelling intensity. The fourth case corresponds to a point source and the fifth case to three equal sources at the position shown. The origin of the horizontal scale in Figure 13 defines the intersection of the valley axis and the line of bridge pillars. Note that the sources have been displaced in the positive direction (downstream, following the valley axis) to account for the pattern of ellipses in Figure 12.

Calculated heave along the viaduct axis is plotted in Figure 14 for the five cases of swelling distribution at depth. It corresponds to the period 26/11/2007–30/04/2008. Also shown in the figure is the measured heave profile of the viaduct for the same time period.

The three continuous distributions reproduce reasonably well the measured heave. Highly concentrated sources (Cases 4 and 5 in Fig. 13) overestimate the maximum heave and reduce the lateral spreading of heave. It is clear that the smoothing effect provided by the thick soil layer above the source area reduces significantly the effect of local variations of swelling sources. Consider, however, the heave experienced by a plane closer to the source area (z = 20 m, in Fig. 15). This is the position of the tip of foundation piles of pillar 5. Now, as expected, the source heterogeneity is readily observed. The piles themselves will introduce an averaging effect that is captured by the model. But they will be affected by a strong heterogeneity of swelling intensity at source level.

The source pattern was inferred by reproducing the three-dimensional heave contours given in Figure 12, following a trial and error procedure. Several distributions of swelling (varying the areas covered with swelling sources and their intensity), all of them having the same total volume change,

were considered for the calculation of ground surface heave. Comparison of calculated heave distribution with field measurements helped to choose an optimum distribution of swelling sources.

Consider the swelling distribution plotted in Figure 16. This distribution has two additive volumes: a uniform expansion in a 100 × 100 m^2 area centred in pile 5 and two rectangular areas whose shapes are inspired by the surface heave pattern. The following volume increments were adopted:

Area 1	100 × 100 m^2	$\Delta V_1 = 60\ m^3$
Area 2	45 × 50 m^2	$\Delta V_2 = 201\ m^3$
Area 3	40 × 45 m^2	$\Delta V_3 = 201\ m^3$

The "continuous" swelling increment is represented by a set of equal spherical sources located at intervals of 1 × 1 m^2 (in plan-view). The calculated surface heave of this swelling source is compared in Figure 17 with measurements. The agreement was estimated to be accurate enough for the main purposes of this work: the effect of heave on the response of the group under pillar 5.

RESPONSE OF PILE GROUP 5. SHORT TERM (5 MONTHS)

The swelling intensity and spatial distribution, assumed to act at a plane located at z = 29 m, was imposed to the foundation of pillar 5 with the help of the program developed. Calculated vertical displacements are given in Figure 18. It can be checked that the pile heads remain in a plane, which is consistent with the hypothesis of a rigid cap. The rotations of the cap with respect to the two axes (x, y) in plan-view were calculated. They are compared with actual measurements in Table 1.

The agreement is remarkable if one considers the complexity and uncertainties of the case. The rotations given in Table 1 are small but they have a non-negligible effect on the bending moments of the pillar and on the pillar-deck connection.

The calculated distribution of vertical loads on the pile group is given in Figure 19. All piles receive different loads from each other. The sum of all calculated loads is equal to the total vertical load

applied by the pillar (27000 kN). The calculated moments on piles along directions x and y (M_x, M_y), as well as the axial forces (F) along the pile length, are given in Figure 20. It is interesting to check how different the reactions of all the piles in the group are. It can be checked that the distribution of moments and normal forces leads in some piles to tensile stresses at the pile head. This issue is further explored in the next section. In fact, the calculation so far refers to a 5-month period in which detailed observations of surface heave, extensometer data, bridge displacements, and pile cap rotations were available. However, the pile foundations of the viaduct have experienced much larger displacements since the end of its construction in September 2002 (Fig. 2).

RESPONSE OF PILE GROUP 5. LONG TERM (5 YEARS)

The available heave data for the long-term (5 years) analysis, given in Figure 2, refers to the upward motion of the pillars observed during levelling the railway tracks. Pillar 5 experienced a heave of 200 mm in the period 09/2002–09/2007. If the pattern of surface heave plotted in Figures 12 or 17 is assumed to be similar over the years the procedure described for the short term period could be extended without major difficulties. In fact, a homothetic increase in volume of the observed heave pattern in Figure 17, leading to a maximum heave of 200 mm (against 36 mm for the short period) in pillar 5 was accepted. The effect of the more intense heaving on the pile group was calculated and the results (M_x, M_y, F) are plotted in Figure 21. Calculated moments are now much larger than the values estimated for the short-term case. They confirm the decisive effect of deep swelling on the loading of individual piles. In two piles (3 and 7) net tensile loads are calculated. The variation of normal forces with depth is far from any intuitive guess for a pile group, essentially subjected to a high vertical load (Fig. 21c). Maximum moments are calculated at the pile-cap interface. Figure 22 is a scheme of the deformation of the pile group.

Unfortunately no measurements of pile cap rotations for the long-term period are available. The calculated rotations are 0.085º and −0.065º in directions x and y. Optical surveys by cameras along borings drilled through the cap and piles in a few cases indicated in all cases a significant fissuring

of the pile-cap contact. This behaviour, which was initially interpreted as an indication of surface swelling can now be explained. In fact, stresses at the pile-cap contact can now be calculated, once the distribution of bending moments and normal forces (Fig. 21) are known. The calculation is summarized in Table 2.

It may be checked that tensile stresses develop in all cases. In seven, out of nine piles, a tensile state is calculated. This is not surprising. In theory, a single pile heaving in a group of piles may lead to tensile stresses in the remaining set of piles. The calculated tensile stresses are high (1 N/mm^2 = 1 MPa) and they are capable of fissuring concrete. Values in excess of 10 MPa are calculated in several piles. These estimations explain a generalized fissuring at the pile-cap contact, a situation which was difficult to explain when it was first observed.

CONCLUSIONS

The heave experienced by a viaduct founded on deep large diameter piles is an extreme case apparently without published precedents. The case led to the interesting foundation problem of determining the reaction of pile groups against a heterogeneous swelling developing at depth.

In order to tackle this problem a calculation procedure has been developed. It integrated some available fundamental solutions, valid for an elastic half space. Some simplifying solutions were adopted to reduce the complexity of the analysis. However, the program developed provides essentially the same response given by other published methods, as well as some 3D analysis performed by finite elements. It offers a fast and friendly calculation procedure, which was useful to perform the analysis described in the paper.

Available extensometer data and surface heave was interpreted with the purpose of estimating the distribution and intensity of the deep swelling, which was due to gypsum crystallization.

The effect of the deep swelling on the analysed pile group is very determinant and modifies substantially the expected group behaviour against the bridge load.

The affected pillars experienced not only an overall heave, but a rotation with components in the direction of the bridge and perpendicular to it. The calculated pile cap rotations are close to field measurements.

The substantial heave experienced in a 5 year period was capable of inducing large bending moments in all piles of a given group. Maximum values are calculated at the pile head. In some piles, tensile loads are calculated despite the vertical load exerted by the bridge. The combination of axial forces and bending moments leads to high tensile stresses in critical pile cross-sections, namely at the pile's head. This explains the generalized concrete fissuring observed by optical cameras in borings drilled through the cap and piles. The explanation given to these observations ruled out any hypothesis of soil swelling along the upper part of pile shafts.

APPENDIX 1. CALCULATION METHOD

The calculation procedure is developed for simplicity for a particular case: The horizontal response of a pile group subjected to horizontal load and the soil expansion.

Consider a pile group of *Np* piles having length *L* and diameter *d* (Fig. 5). The piles are connected by a rigid pile cap, so that the pile heads remain always on a plane. Figure 5 shows the set of horizontal loads applied to the pile group and the increment in volume of a point within the soil located in a given point of coordinates (x, y, h). Horizontal stresses (f_h) act on the soil surface. Consider the calculation procedure for the case of a pile group loaded by a horizontal load F_y.

The external force applied to the pile group is first distributed among the piles of the group. The two horizontal forces are saved in a matrix (*Np* x 2), where each line represents the force acting on one single pile. Piles are subdivided into a number of elements N_E. For each pile a (N_E x 2) matrix is created. Each line represents the coordinates of the centre of pile elements.

Consider the displacements of piles in horizontal direction (x-direction or y-direction). They are described by the following relationship:

$$[D] \cdot \{\rho_P\} + \{B_P\} = [A_P] \cdot \{p\} \quad (1)$$

where

$\{\rho_P\}$ is the ((N_E x N_P) x 1) column vector of pile elements displacements

$\{p\}$ is the ((N_E x N_P) x 1) column vector of interaction stress (p_{ij} in Fig. 5)

$[D]$ is the ((N_E x N_P) x (N_E x N_P)) matrix that contains the finite difference coefficients arising from the discretization of the differential equation describing the bending of piles (Poulos and Davis, 1980)

$\{A_P\}$ is the ((N_E x N_P) x (N_P)) matrix that contains the coefficients derived from the equilibrium conditions for loads applied to each individual pile

Soil displacements for all points along the piles are calculated as a superposition of the soil displacements due to the horizontal loading between soil and pile (Mindlin, 1936), the displacements resulting from the distributed load applied at the surface (Boussinesq, 1885) and the displacements due to the volumetric expansion (Sagaseta, 1987). Therefore:

$$\{\rho_S\} = [A_S] \cdot \{p\} + \{\rho_{Boussinesq}\} + \{\rho_{Expansion}\} \quad (2)$$

where

$\{\rho_S\}$ is the (N_E x N_P) column vector of the horizontal soil displacements

$[A_S]$ is the ((N_E x N_P) x (N_E x N_P)) matrix of soil-displacement-influence factors obtained from the integration of the Mindlin (1936) fundamental solution

$\{\rho_{Bousinesq}\}$ is the ((N_E x N_P) x 1) horizontal soil displacement column vector due to the distributed horizontal load f_h at the surface calculated according to Boussinesq (1885)

$\{\rho_{Expansion}\}$ is the ((N_E x N_P) x 1) horizontal soil displacement column vector due to the volumetric expansion of soil.

The system of equations (1) and (2) for the pile and the soil structure is solved by imposing compatibility of displacements between soil and pile:

$$\{\rho_S\} = \{\rho_P\} \quad (3)$$

Equations (1), (2) and (3) provide:

$$\{p\} = ([A_P] - [D] \cdot [A_S])^{-1} \cdot \left([D] \cdot \left(\{\rho_{Expansion}\} + \{\rho_{Boussinesq}\}\right) + \{B_P\}\right) \quad (4)$$

$\{\rho_{Expansion}\}$ is calculated by means of Sagaseta (1987) solution. The horizontal displacements, induced by a volumetric increment, ΔV, characterized by a sphere or radius a ($\Delta V = 4/3\ \pi a^3$), are given by

$$\rho_{Expansion} = u = -\frac{a^3}{3}\left(\frac{x}{{r_1}^3} - \frac{x}{{r_2}^3}\right) \quad (5)$$

where

$$r_1 = (x^2 + (z - h)^2)^{1/2}$$

$$r_2 = (x^2 + (z + h)^2)^{1/2}$$

z: depth of the point where displacement is calculated. At surface z=0

h: depth of the expanding source

x: horizontal distance between the source and the point where soil displacements are calculated

The solution (5) corresponds to the "paved half-space" case (Sagaseta, 1987), which is sufficiently accurate in our case because the soil expansion occurs in a volume located at relatively large depths, varying between 20 and 30m.

The vertical displacements and forces in the pile group shown in Figure 4 are calculated following a similar procedure. As before, the compatibility between vertical displacements of soil and pile elements leads to a set of algebraic equations allowing the calculation of pile displacements. The Sagaseta (1987) solution for vertical displacements in a paved half-space,

$$w = -\frac{a^3}{3}\left(\frac{z-h}{{r_1}^3} - \frac{z+h}{{r_2}^3}\right) \quad (6)$$

is used in this case to calculate the vertical displacements. Note that in a general case additional cross terms providing horizontal/vertical displacements due to vertical/horizontal loads should be introduced.

ACKNOWLEDGEMENTS

The National Agency for Railway Infrastructure (ADIF) provided technical support during the development of the work reported in the paper. Special thanks are given to ADIF engineers R. Rodríguez, J. García-Germán, S. Martínez Priego and A. Alba.

REFERENCES

Alonso, E. E. and Ramon, A. (2013). Heave of a railway bridge induced by gypsum crystal growth: field observations. *Géotechnique* **63**, No. 9, 707 – 719, [http://dx.doi.org/10.1680/geot.12.P.034]

Boussinesq, J. (1885). Applications des potentiels à l'etude de l'equilibre et du mouvement des solides élastiques, Paris, Gauthier-Villard.

Jiménez-Salas, J. A. and J. A. Belzunce (1965) Resolution théorique de la distribution des forces dans des pieux. Proc. 6th Int Conf. on Soil Mech. and Found. Eng., Montreal, Vol. II, 309-313.

Kovári, K. & Amstad, C. (1982). A new method of measuring deformations in diaphragm walls and piles, *Géotechnique* **32**, No. 4, 402–406, http://dx.doi.org/10.1680/geot.1982.32.4.402.

Mindlin, R. D. 1936. Force at a point in the interior of a semi-infinite solid. Journal of Applied Physics, 7: 195–202.

Nelson, J. D. & Miller, D. J. (1992). Expansive soils. Problems and practice in foundation and pavement engineering. John Wiley & Sons, New York.

Poulos, H.G. & Davis, E.H. (1980). Pile foundation analysis and design. John Wiley & Sons, New York.

Ramon, A and Alonso, E. E. (2013). Heave of a railway bridge: modelling gypsum crystal growth. *Géotechnique* **63**, No. 9, 720 – 732, [http://dx.doi.org/10.1680/geot.12.P.035]

Sagaseta, C. 1987. Analysis of undrained soil deformation due to ground loss. Géotechnique, 37: 301–320.

LIST OF TABLES

TABLES

Table 1: Rotation angles (º) calculated with CANDÍ and values measured in the cap of piles of pillar 5 in the period 21/11/2007–25/04/2008.

Slope direction	Calculated (CANDÍ)	Measured
x	0.0155	0.0176
y	0.0119	0.091

Table 2: Normal stresses (maximum tensile and minimum in compression) at pile head along directions x and y. Heave period: 09/2002–09/2007. Pillar 5.

Pile	Axial force (kN)	M_x (kN·m)	M_y (kN·m)	σ_x (*) (N/mm^2)	σ_y (*) (N/mm^2)
1	2854	–7860	977	–16,49	–0,88
2	7498	–2071	–25	–1,19	3,45
3	–4311	4356	–1353	–11,89	–5,08
4	2279	–8638	2842	–18,52	–5,38
5	10136	–3300	1857	–2,74	0,53
6	2504	2784	506	–5,14	–0,02
7	–4131	–9432	4109	–23,32	–11,25
8	7361	–4412	3211	–6,56	–3,84
9	2810	1443	1970	–1,96	–3,15

(*) Sign – indicates tension; sign + indicates compression

LIST OF FIGURES

Figure 15: Vertical displacements calculated at the depth of the tip of piles (z=20m) due to swelling sources with different configuration

Figure 16: Distribution of the areas of application of swelling for the calculation of the pile group

Figure 17: Measured heave at ground surface (discontinuous lines) and calculated (continuous lines)

Figure 18: Calculated heave at the head of piles. Swelling period: 5 months

Figure 19: Calculated vertical loads at the head of piles. Swelling period: 5 months

Figure 20: Calculated bending moments and axial forces in piles. Swelling period: 5 months

Figure 21: Bending moments and axial force. M_x: rotation around axis Y and; M_y: rotation around x axis

Figure 22: Sketch of the pile group calculated deformation due to swelling

FIGURES

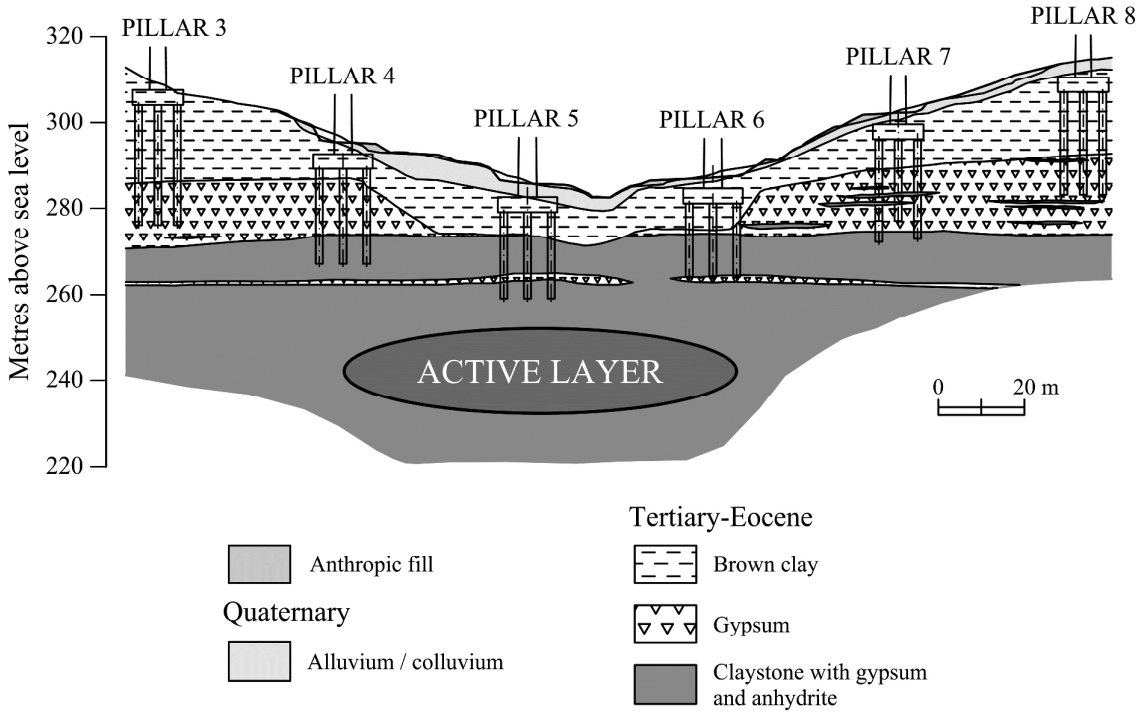

Figure 1: Geological profile along bridge axis

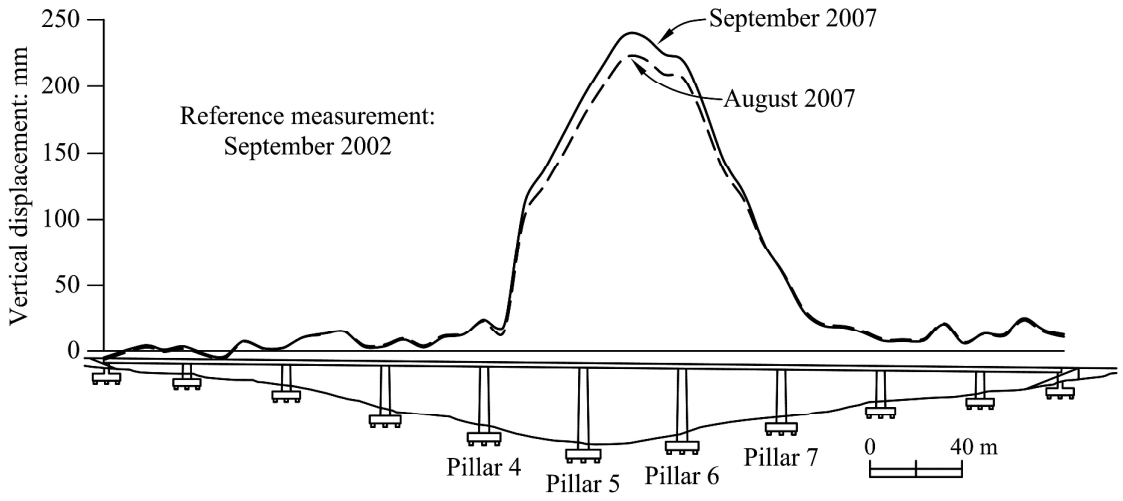

Figure 2: Heave profiles measured in August and September 2007. Initial reading: September 2002

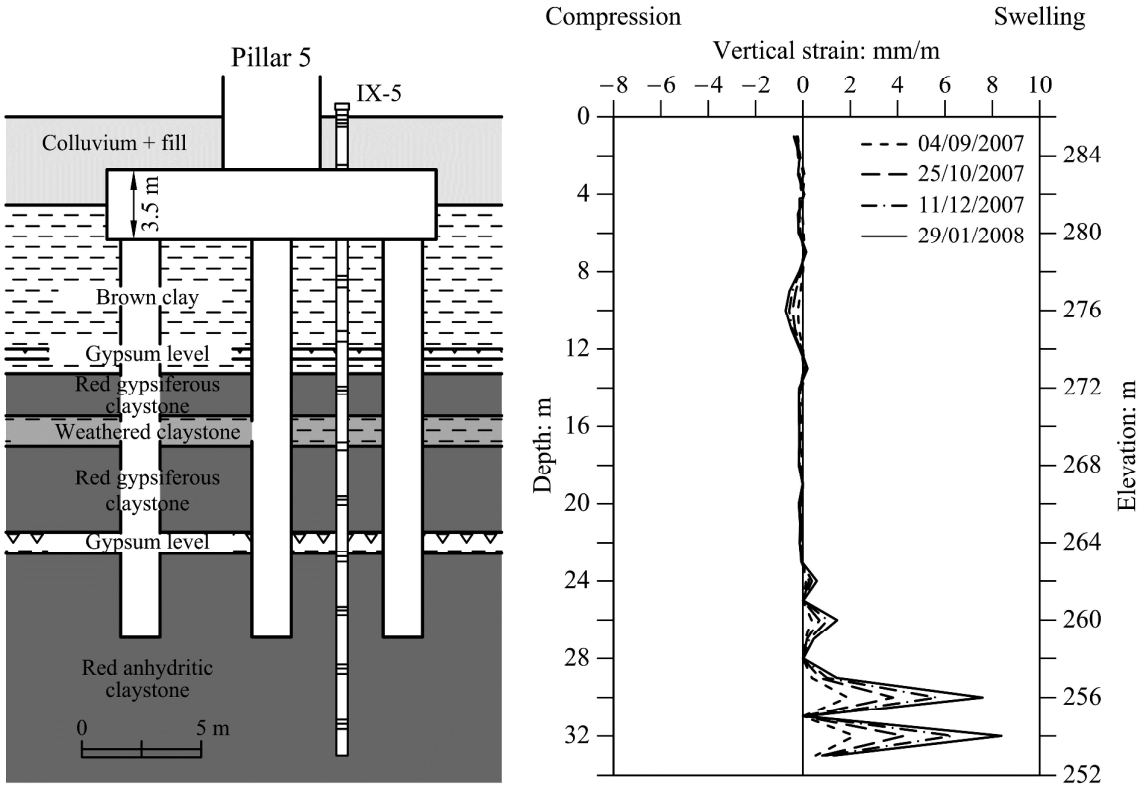

Figure 3: Strains measured in extensometer IX-5 from 4 September 2007 and 29 January 2008. Initial reading: 12 July 2007

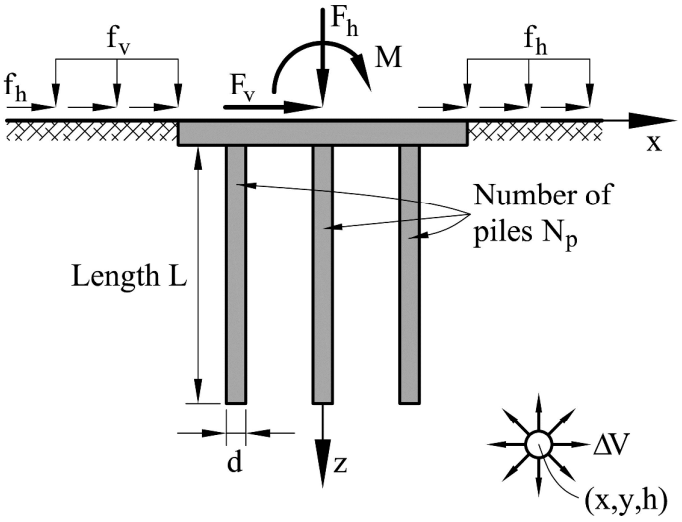

Figure 4: Sketch of the problem analysed

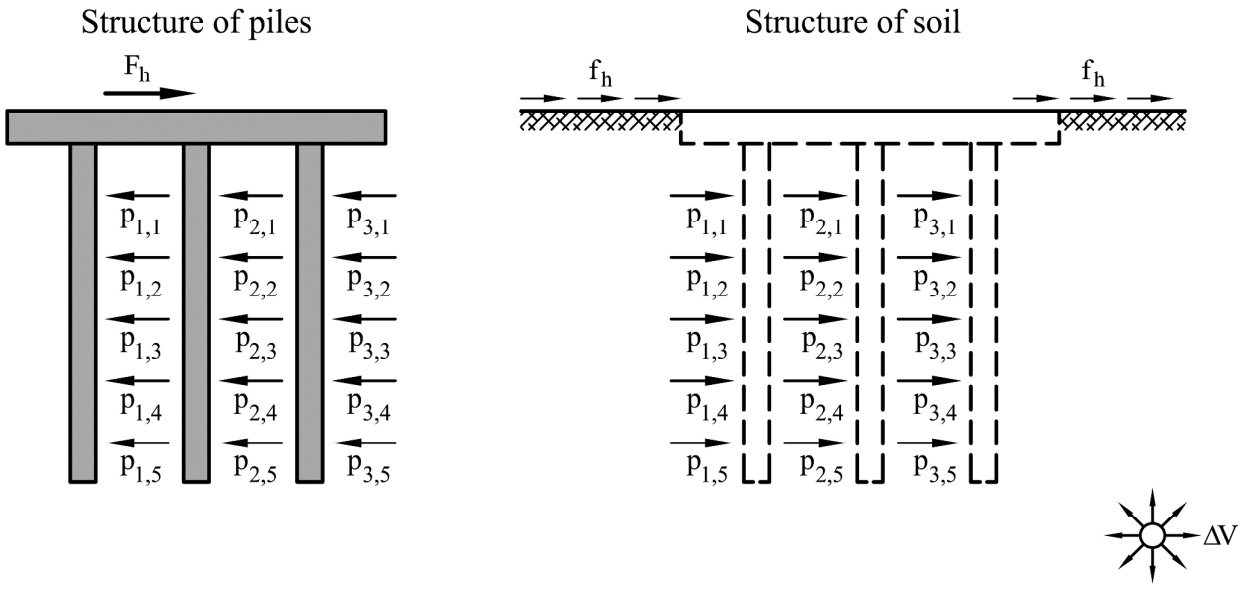

Figure 5: The two “structures” of the problem: the pile group and the ground

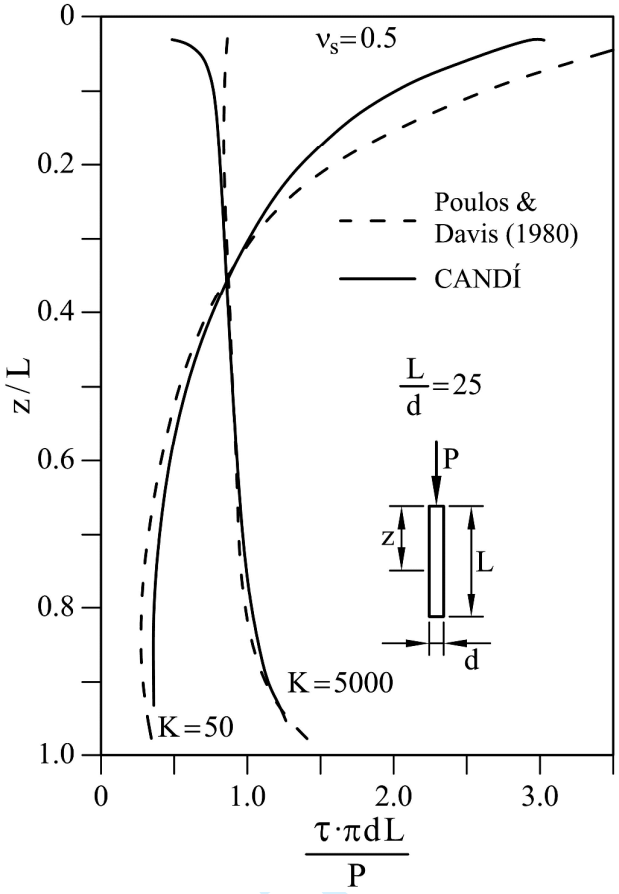

Figure 6: Normalised shear stress along the shaft of the pile for a single pile under vertical load

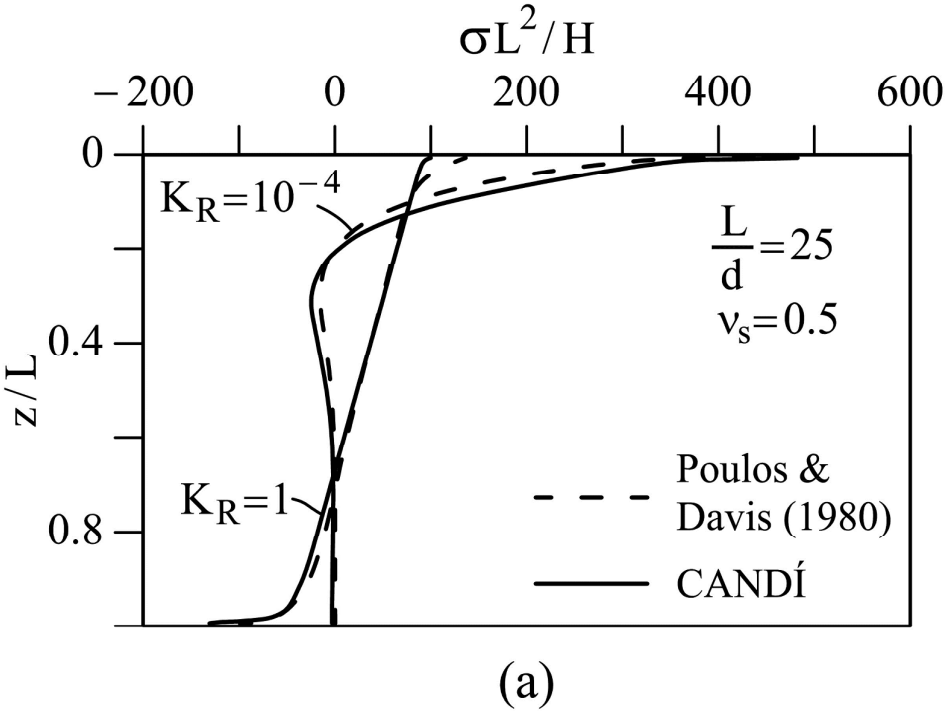

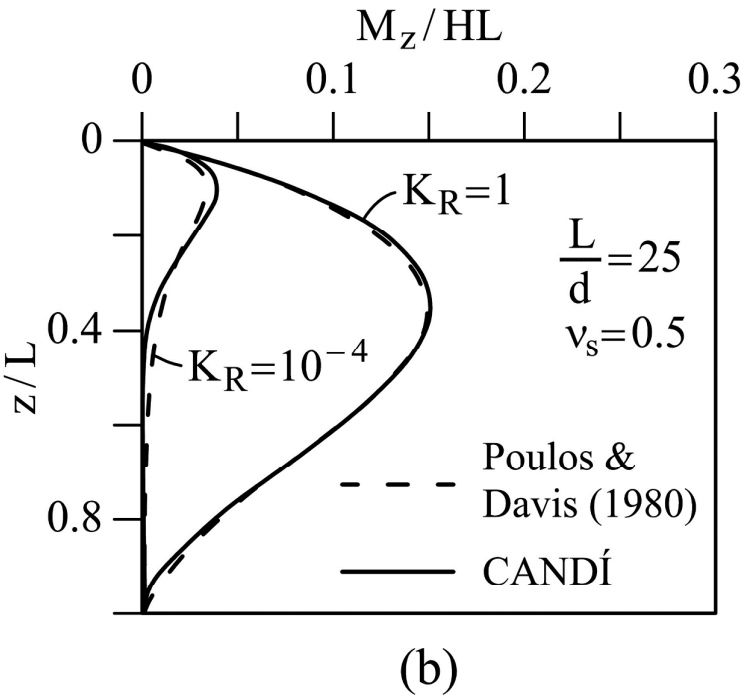

(b)

Figure 7: Comparison of the normalised results of the calculus of a single pile under horizontal load at the top and free pile head: (a) lateral earth pressure; (b) bending moment

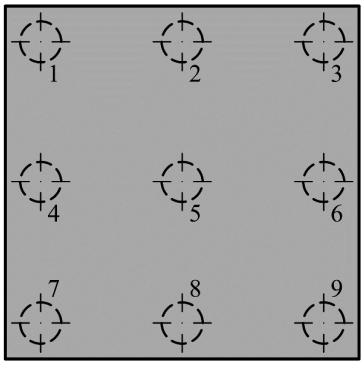

(a)

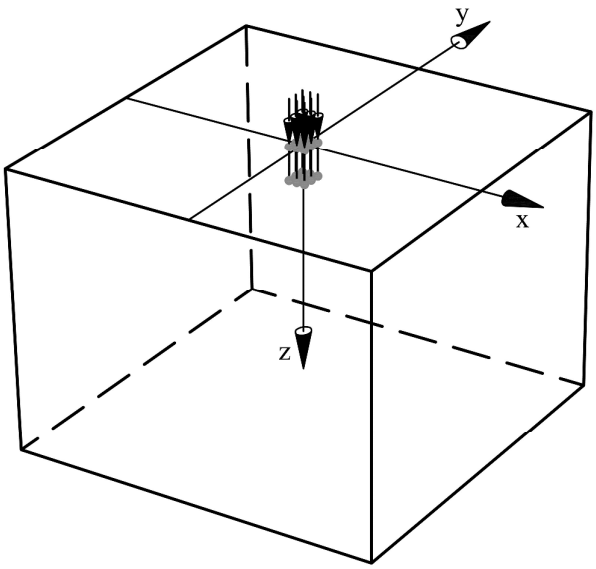

(b)

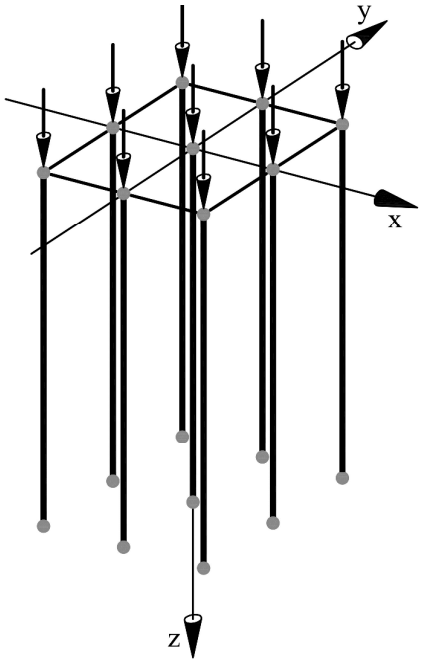

(c)

Figure 8: Plaxis 3D model: (a) pile numbering; (a) global view; (c) piles detail

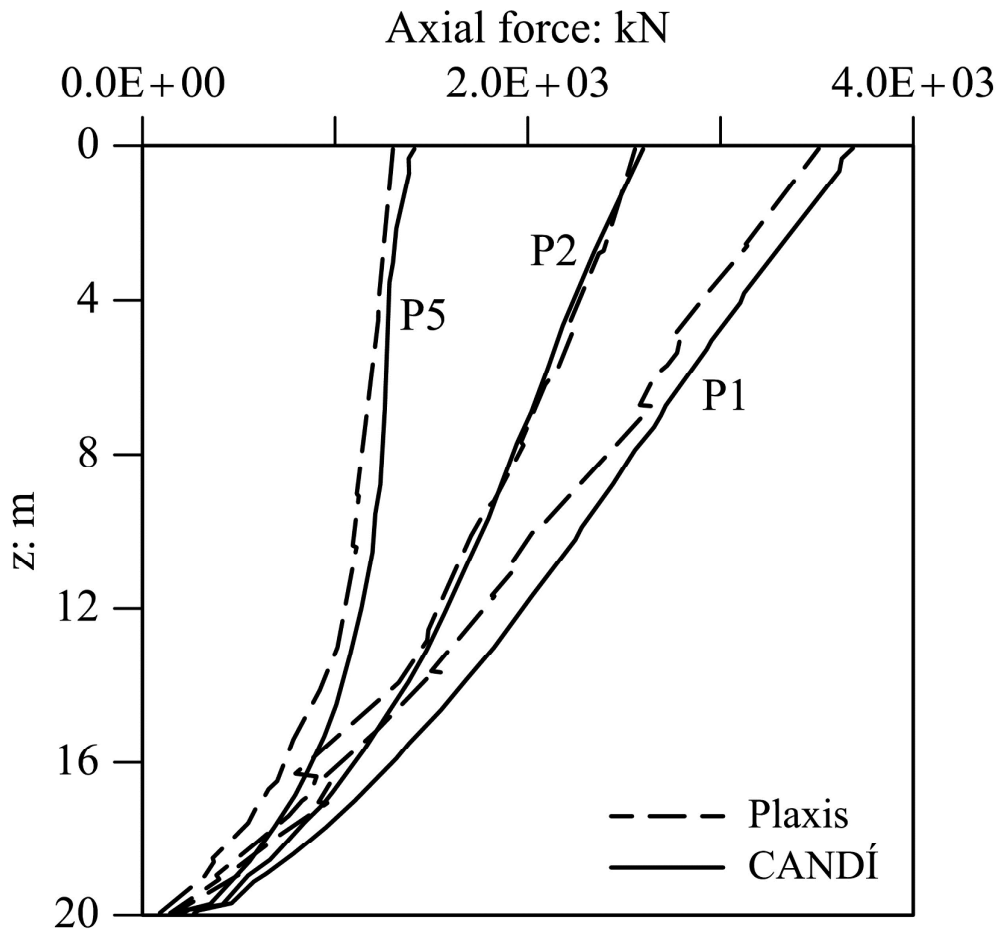

Figure 9: Axial forces calculated along piles P1, P2 and P5 (Figure 8(a)) of a group of piles with pile-cap

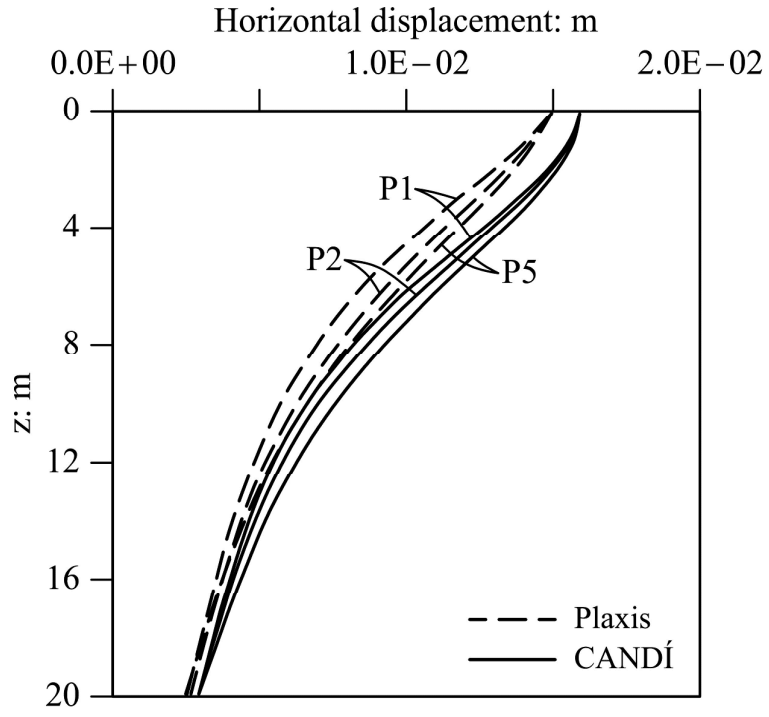

(a)

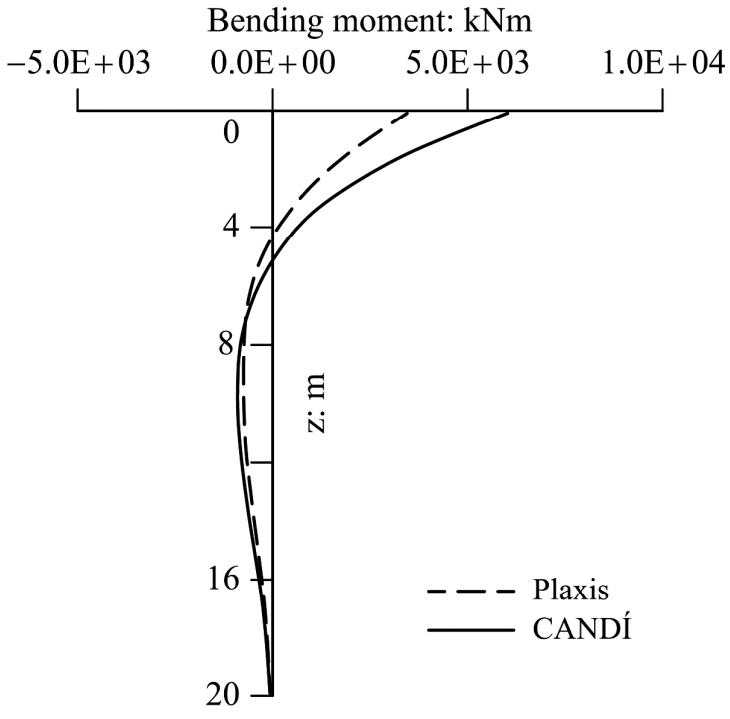

(b)

Figure 10: Comparison of the distribution of (a) horizontal displacements of a group of piles with rigid pile-cap; and (b) bending moments along the shaft of Pile 5 (Figure 8(a)), calculated with Plaxis and CANDÍ

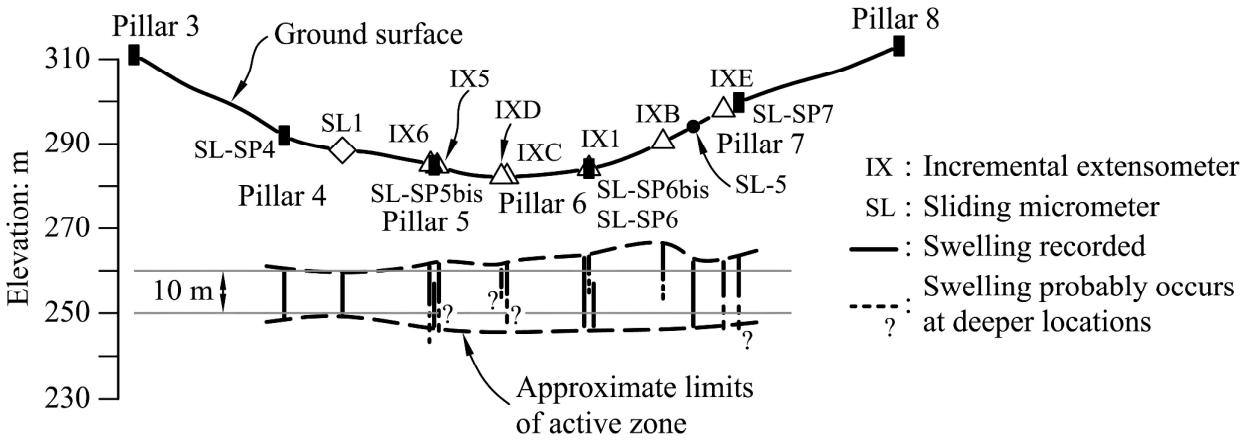

Figure 11: Distribution of the zone with swelling measurements at the valley (Alonso & Ramon, 2013)

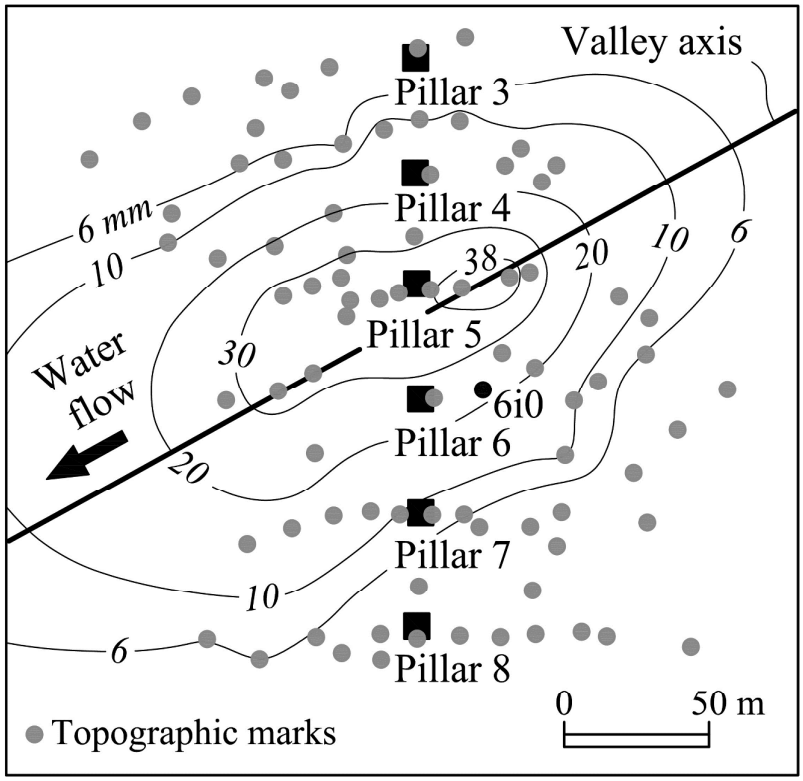

Figure 12: Heave measurements at ground surface from 26 November 2007 to 30 April 2008 (Alonso & Ramon, 2013)

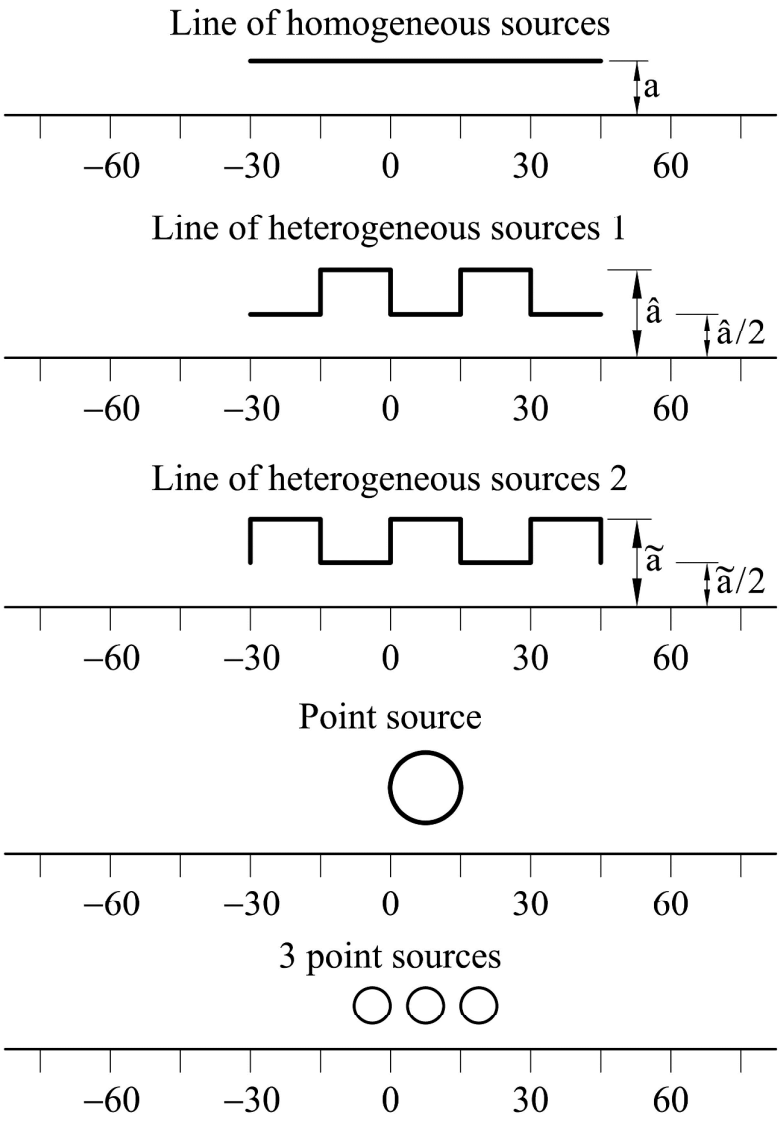

Figure 13: Distribution of swelling sources in the analysed cases

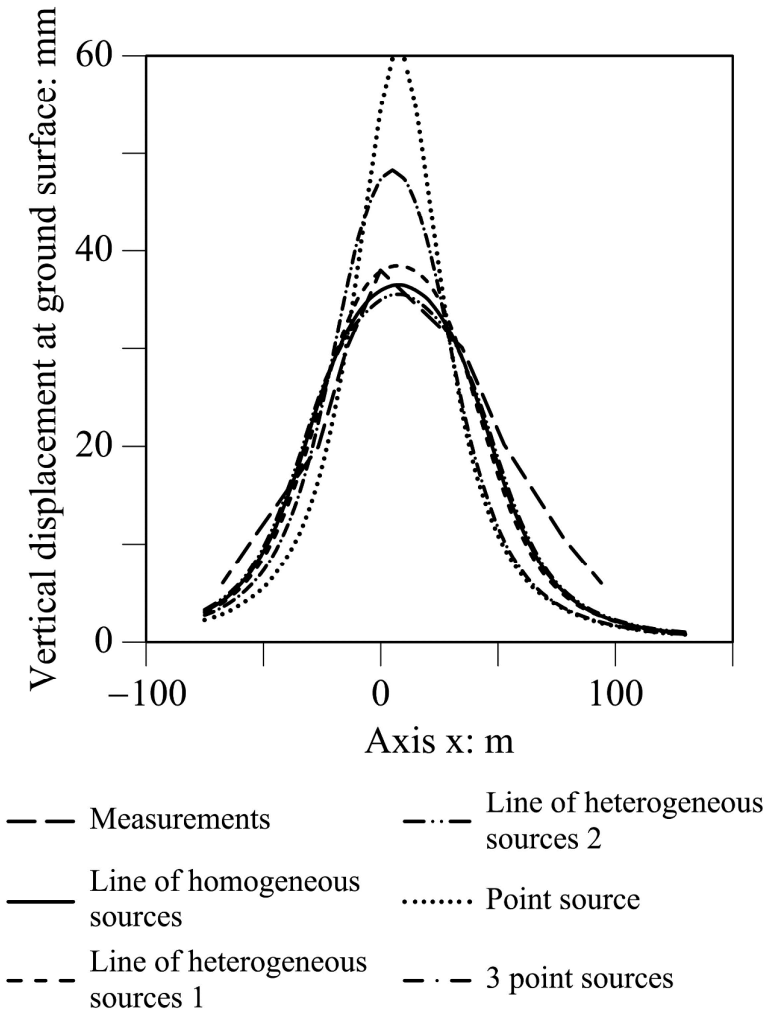

Figure 14: Vertical displacements measured and calculated at ground surface due to swelling sources with different configuration

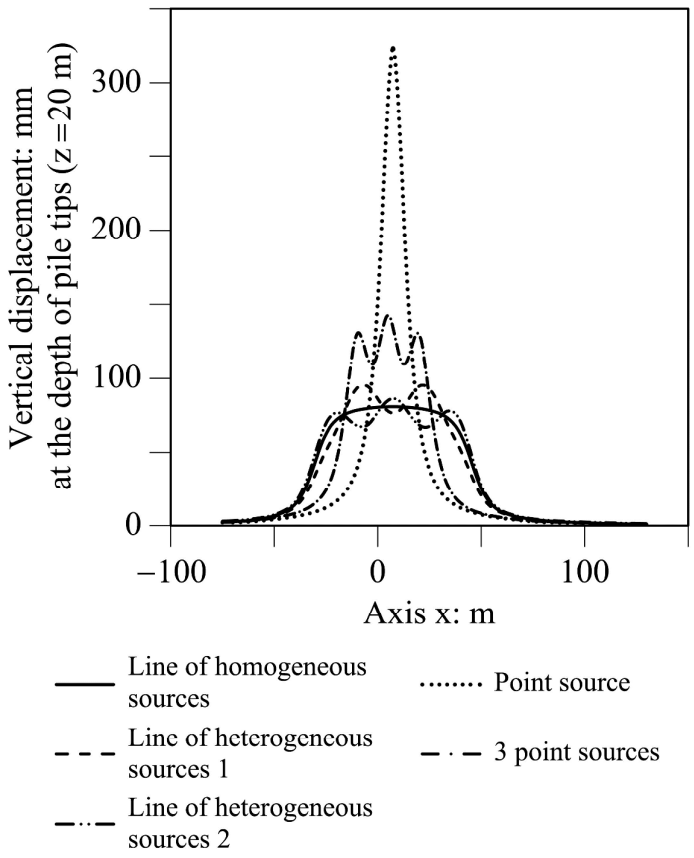

Figure 15: Vertical displacements calculated at the depth of the tip of piles (z=20m) due to swelling sources with different configuration

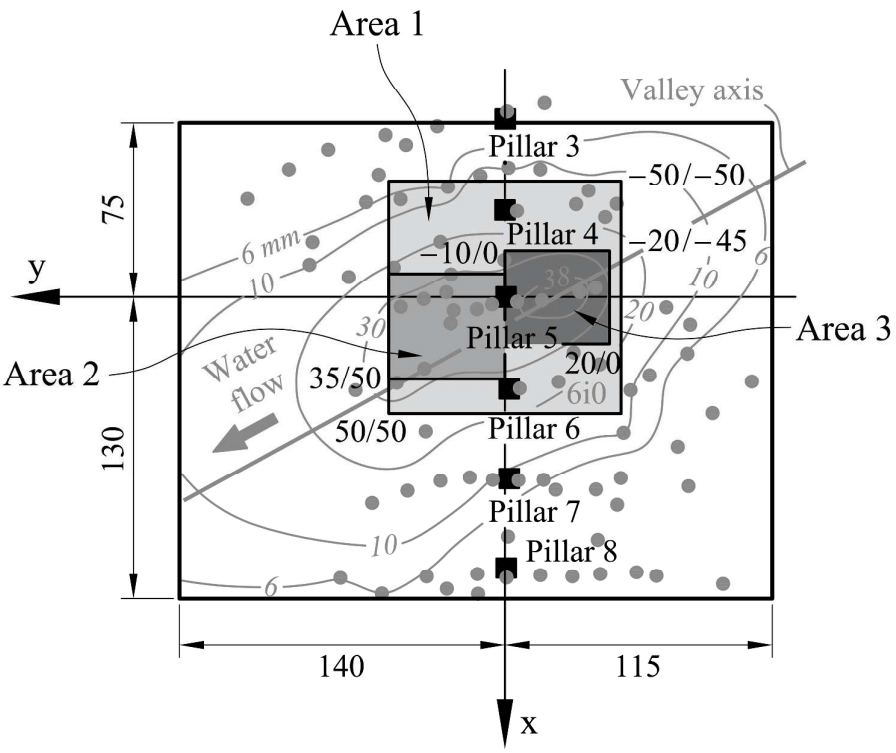

Figure 16: Distribution of the areas of application of swelling for the calculation of the pile group

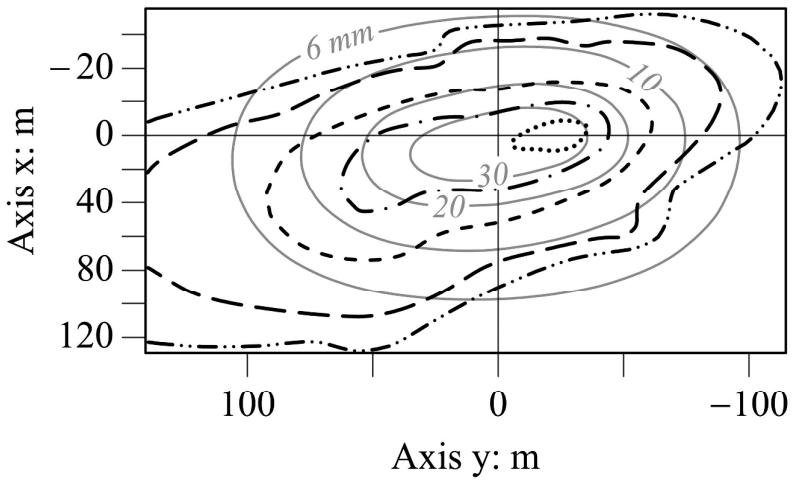

Figure 17: Measured heave at ground surface (discontinuous lines) and calculated (continuous lines)

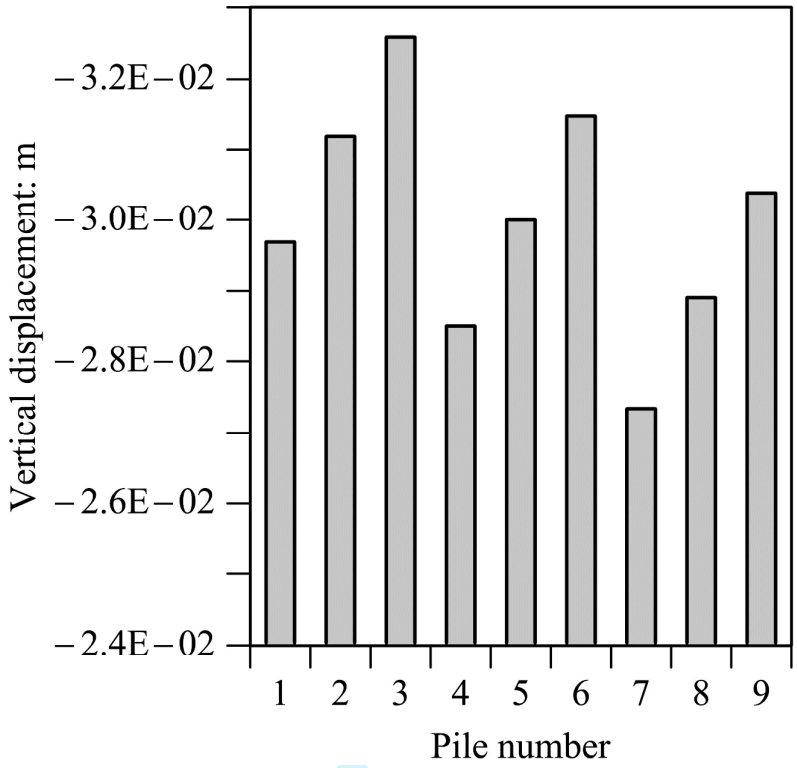

Figure 18: Calculated heave at the head of piles. Swelling period: 5 months

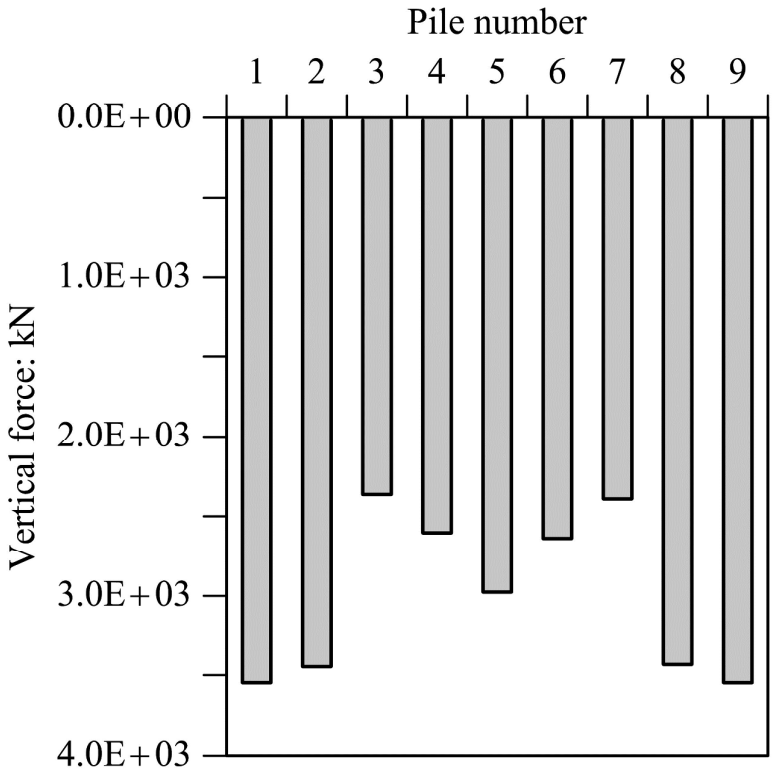

Figure 19: Calculated vertical loads at the head of piles. Swelling period: 5 months

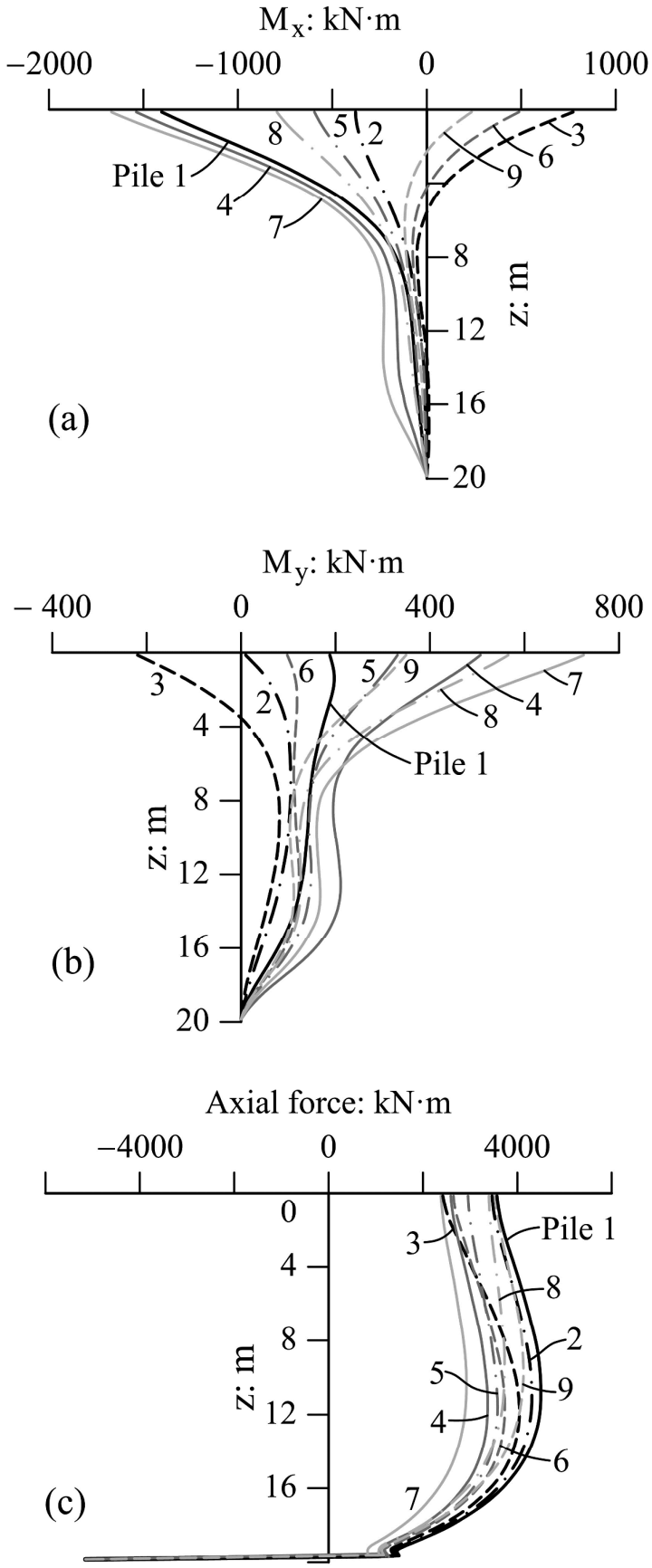

Figure 20: Calculated bending moments and axial forces in piles. Swelling period: 5 months

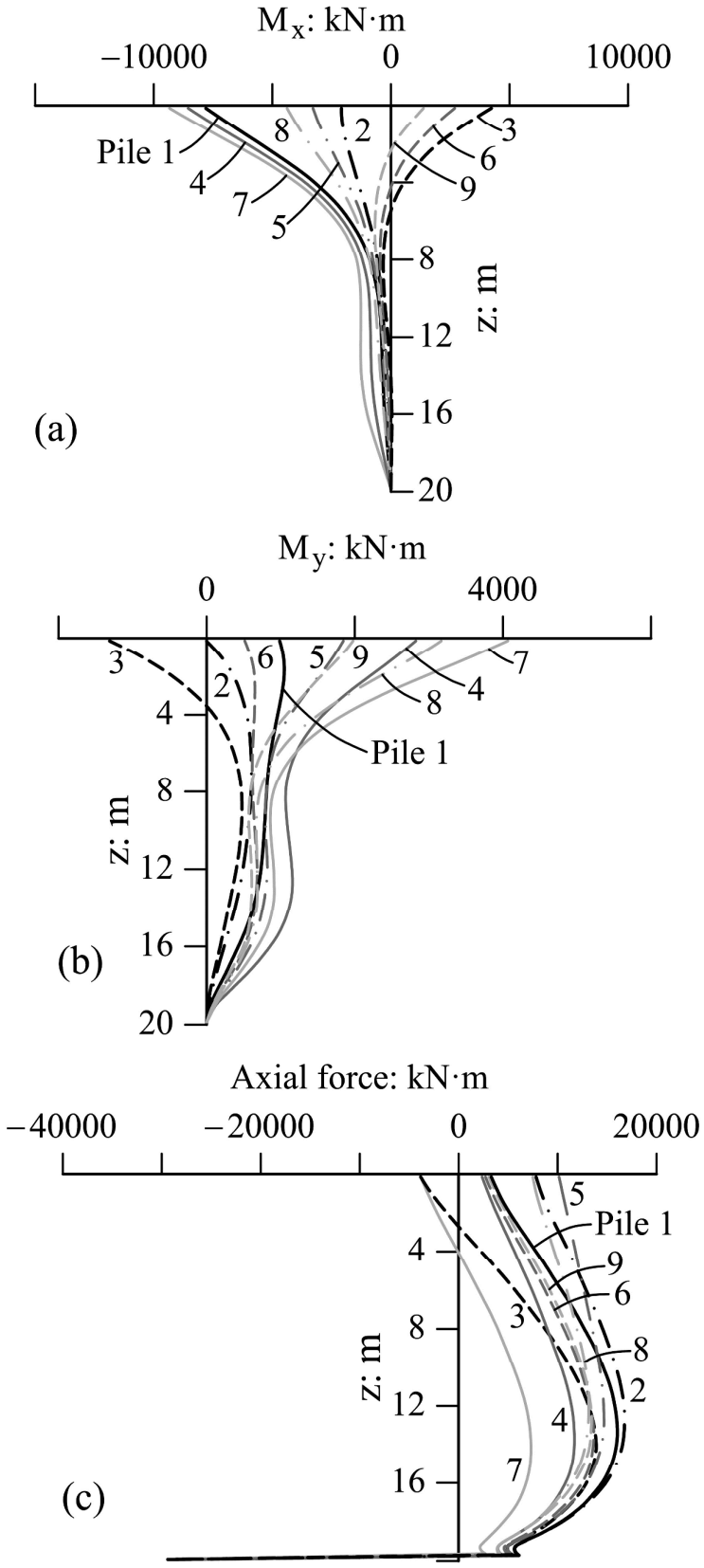

Figure 21: Bending moments and axial force. M_x: rotation around axis Y and; M_y: rotation around x axis

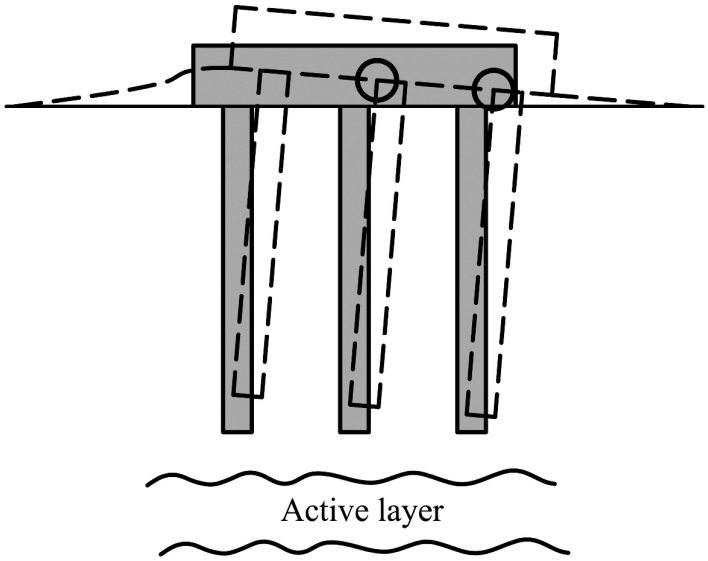

Figure 22: Sketch of the pile group calculated deformation due to swelling

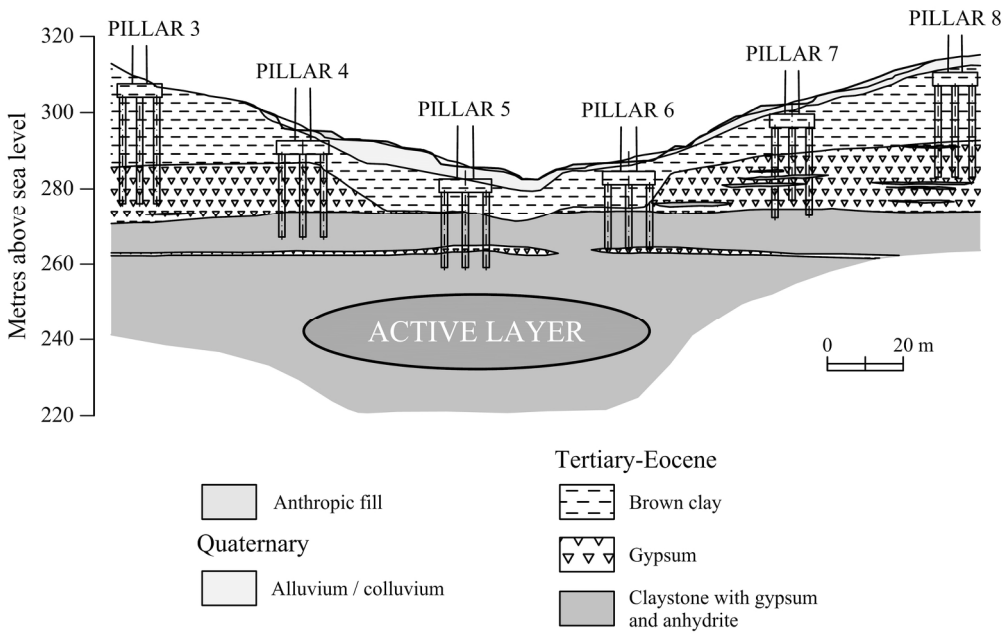

93x58mm (600 x 600 DPI)

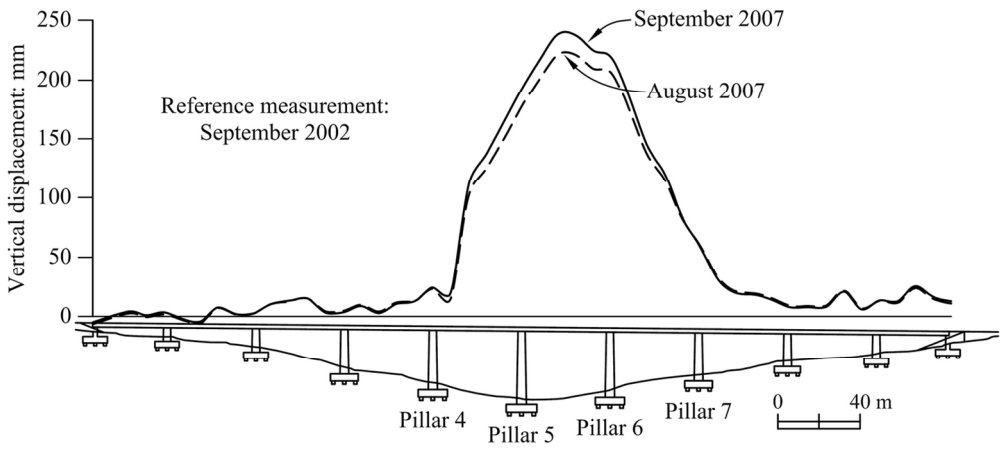

62x27mm (600 x 600 DPI)

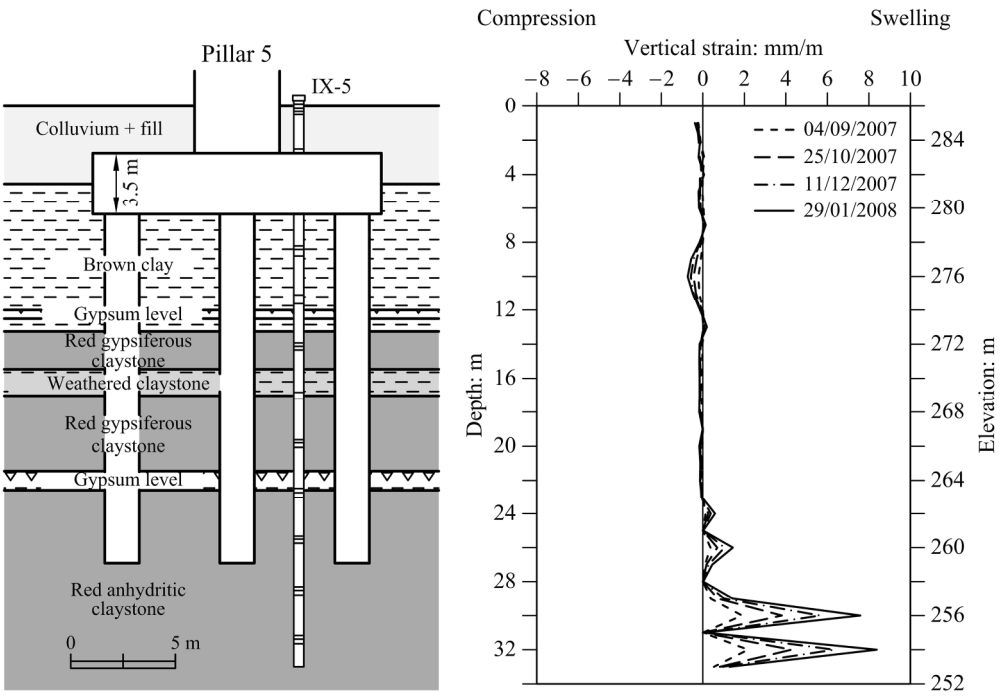

99x68mm (600 x 600 DPI)

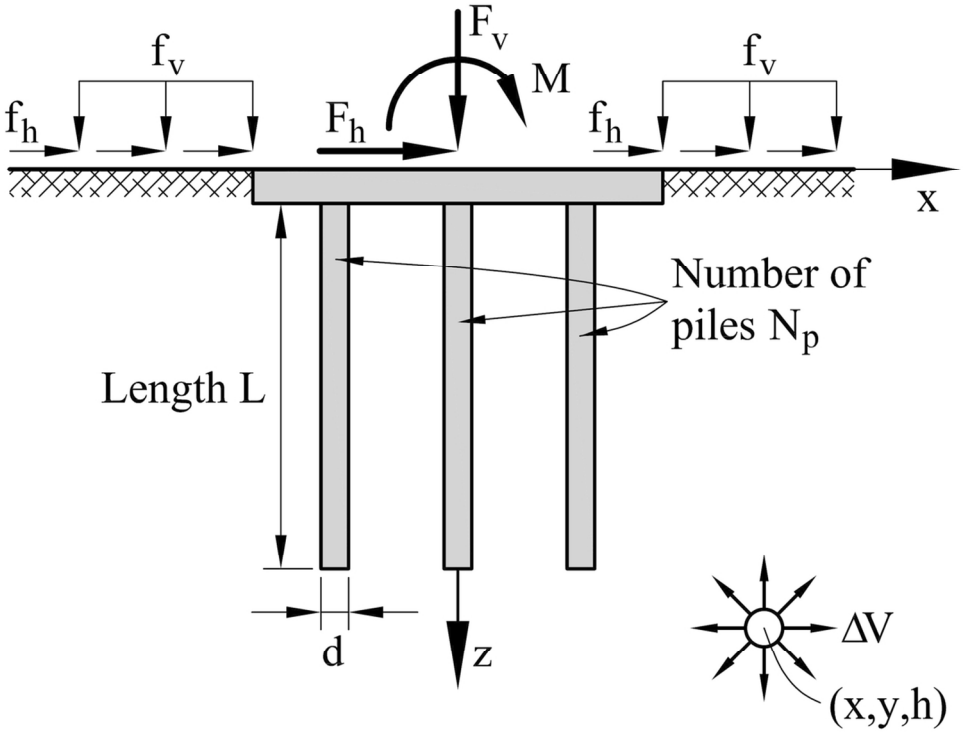

55x42mm (600 x 600 DPI)

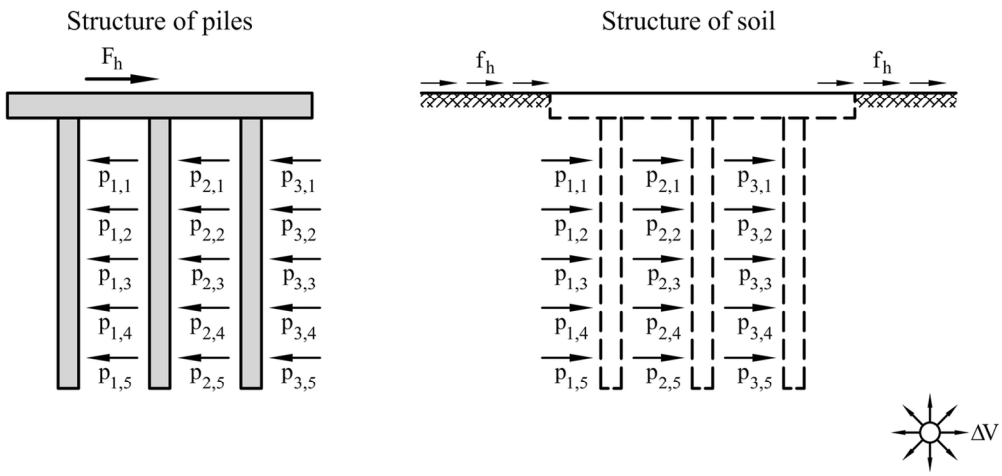

64x30mm (600 x 600 DPI)

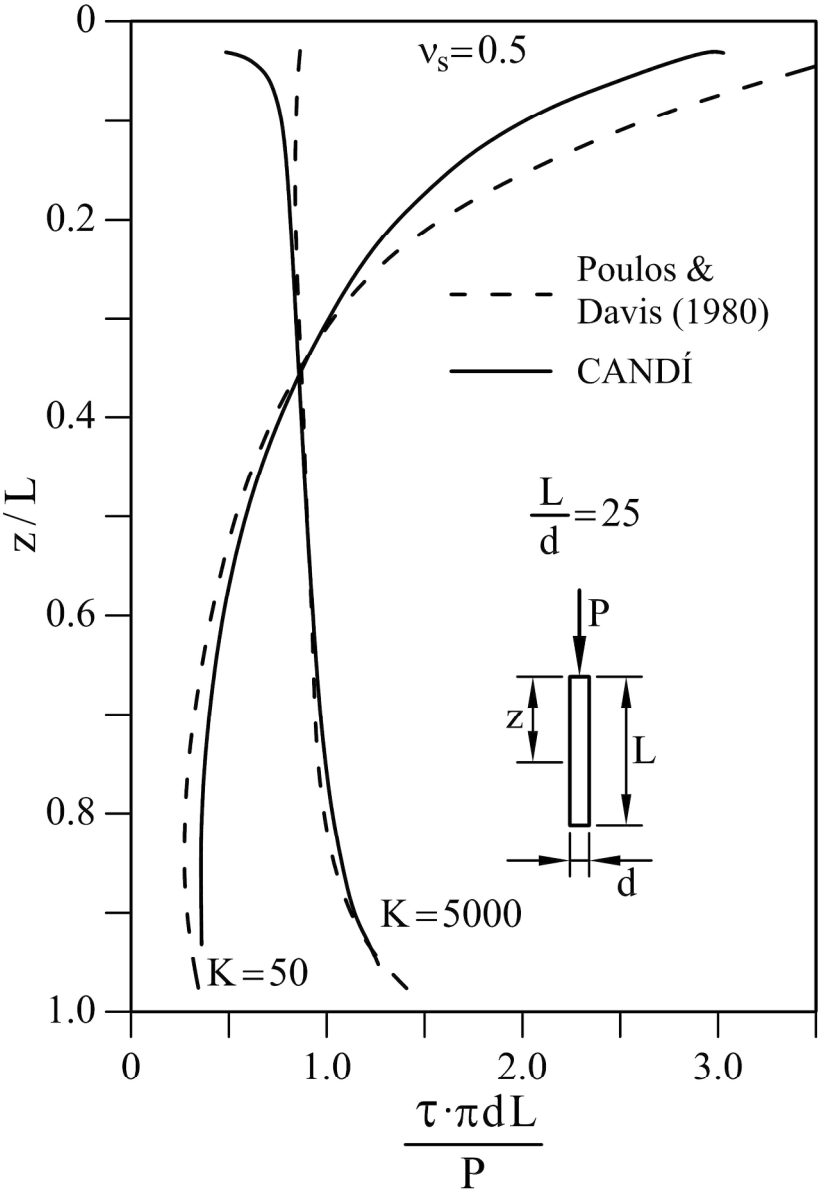

96x139mm (600 x 600 DPI)

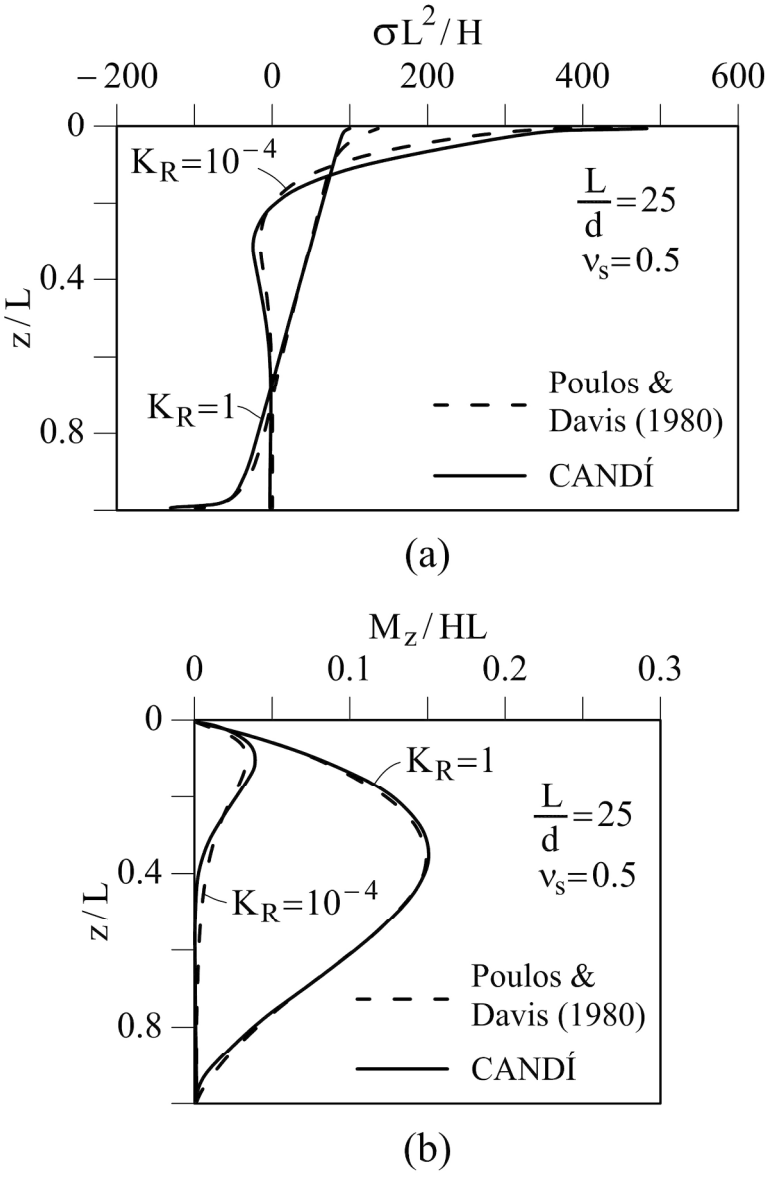

106x159mm (600 x 600 DPI)

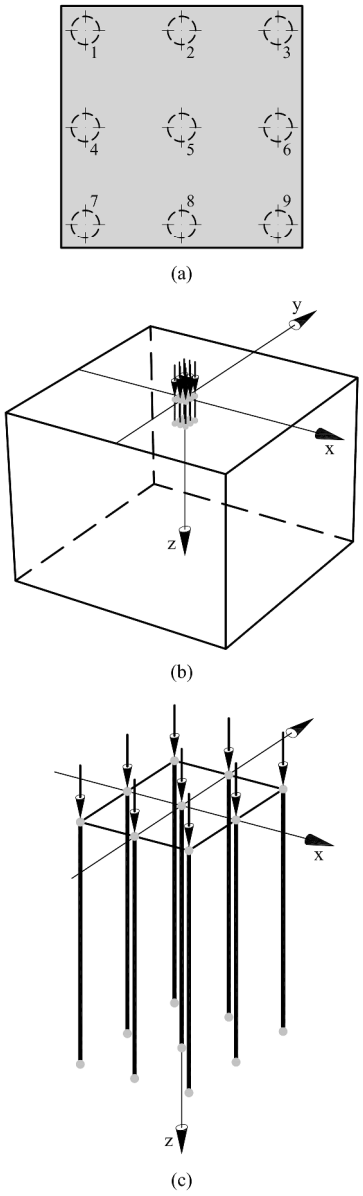

228x742mm (600 x 600 DPI)

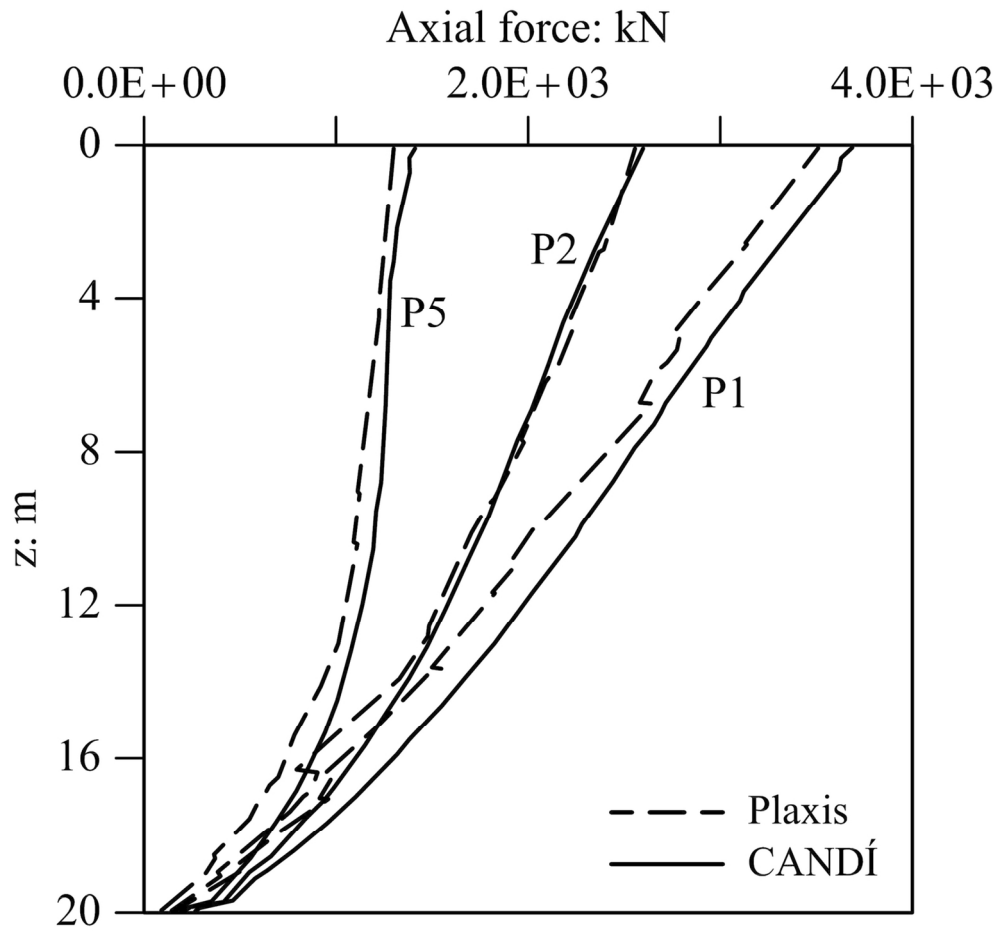

67x62mm (600 x 600 DPI)

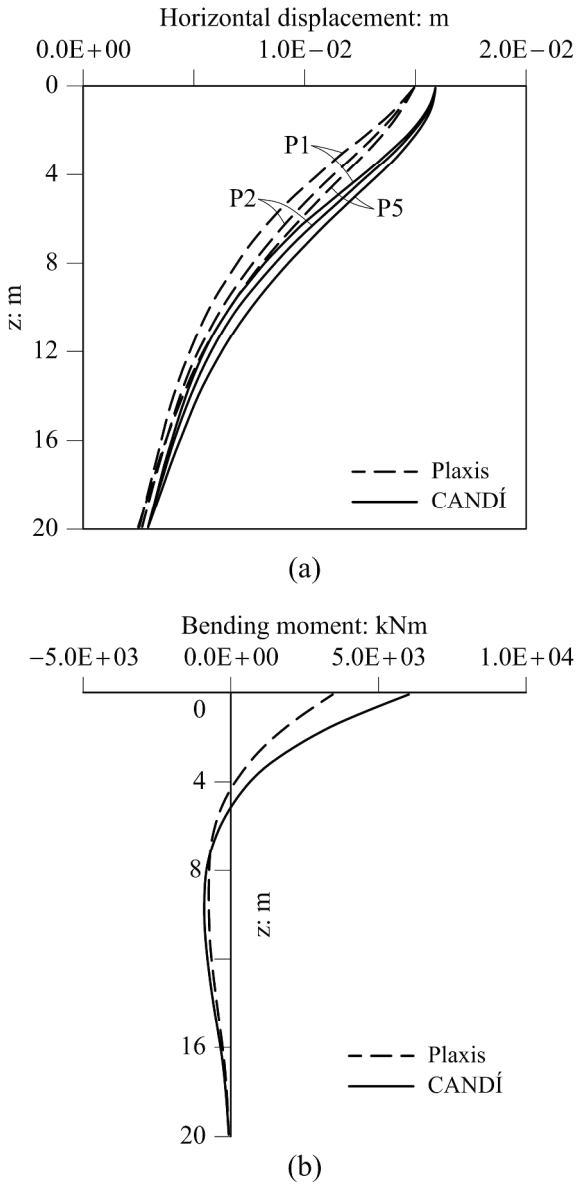

148x301mm (600 x 600 DPI)

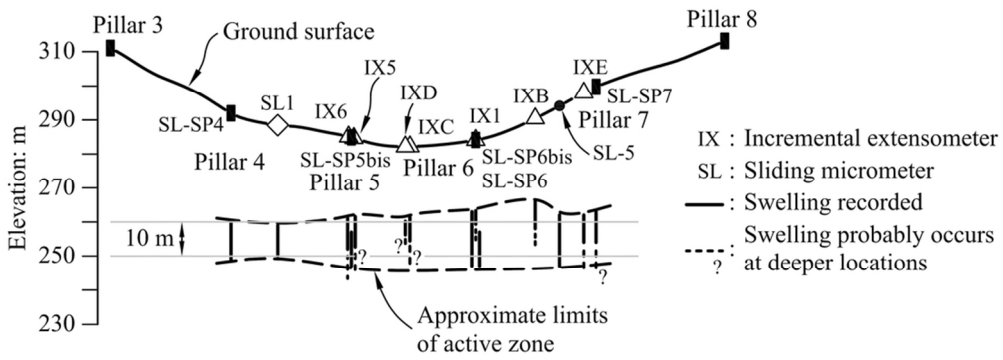

46x16mm (600 x 600 DPI)

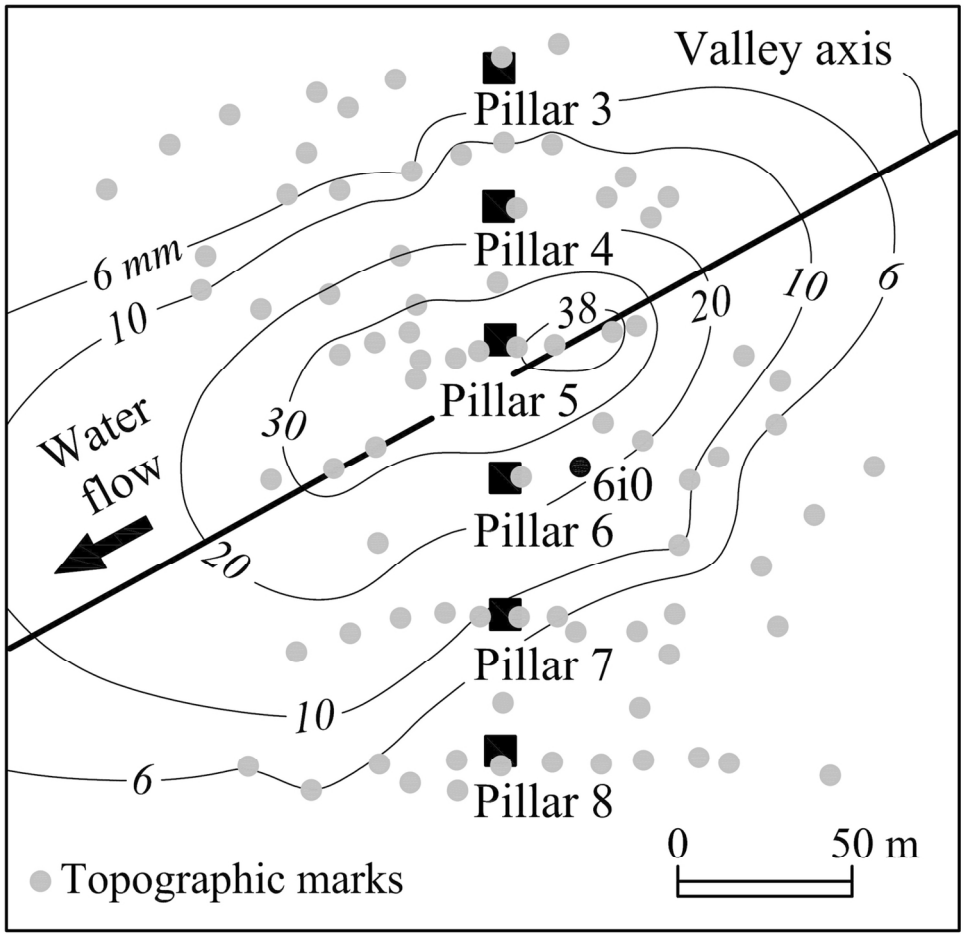

65x63mm (600 x 600 DPI)

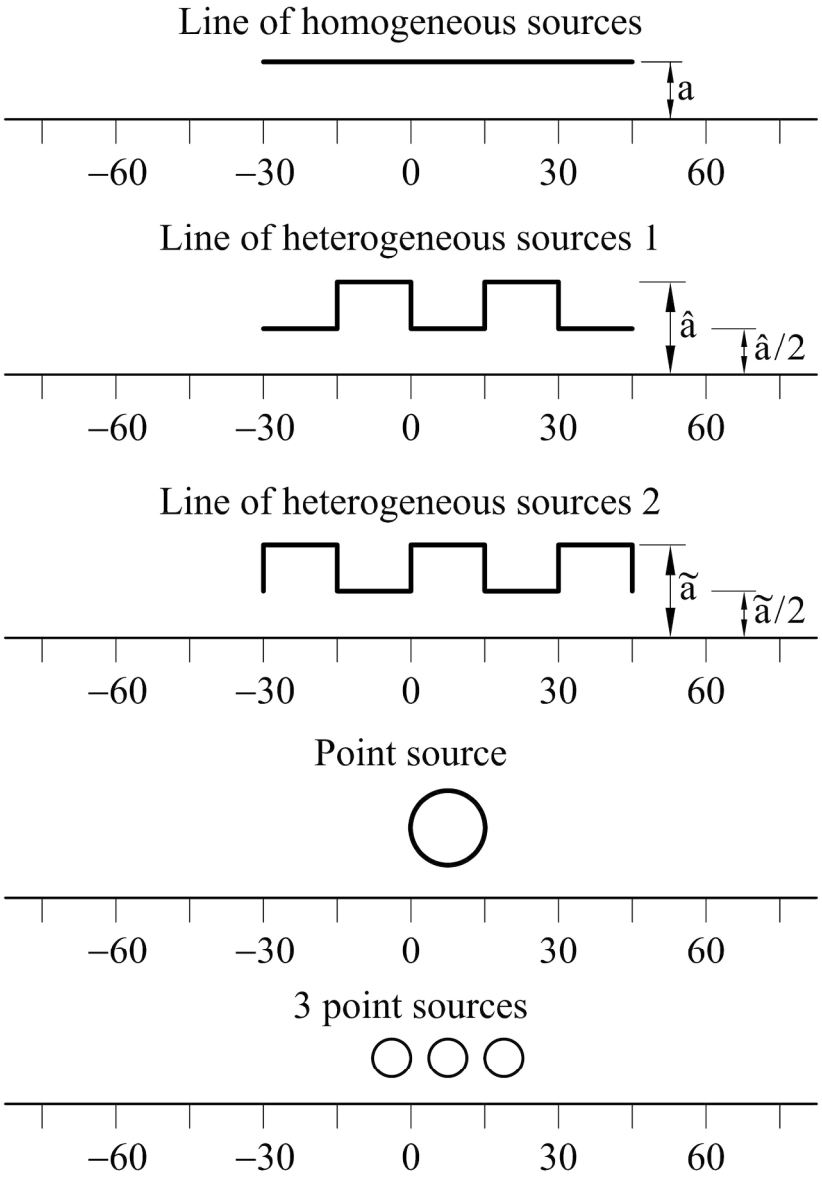

100x141mm (600 x 600 DPI)

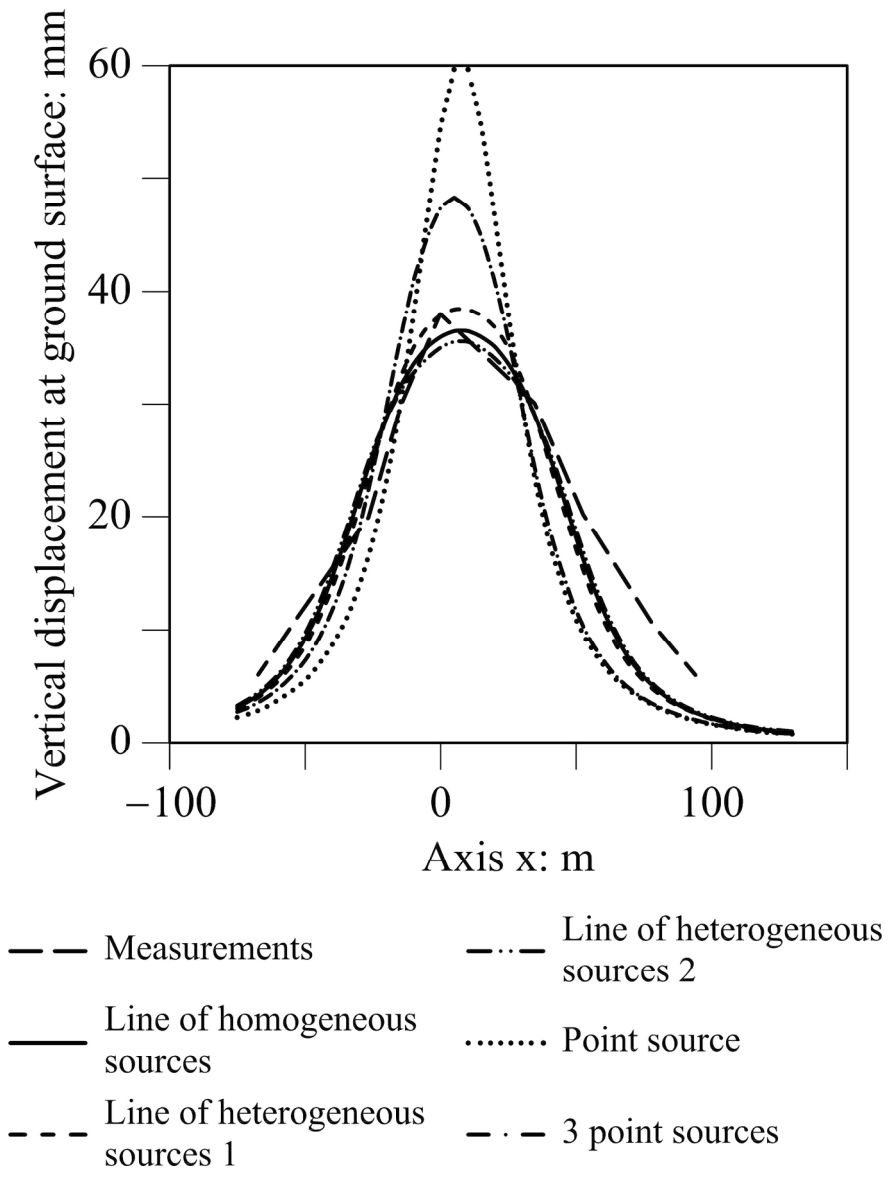

88x116mm (600 x 600 DPI)

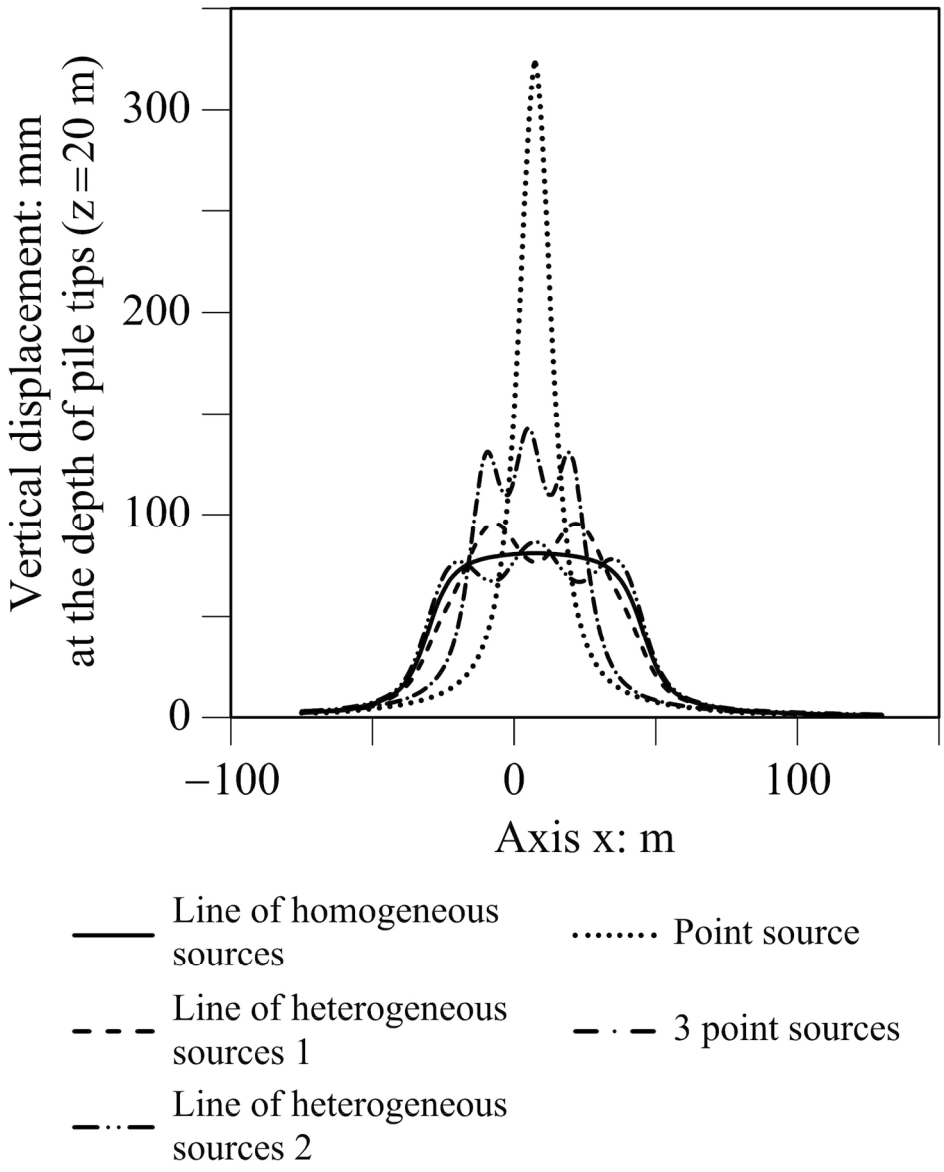

84x103mm (600 x 600 DPI)

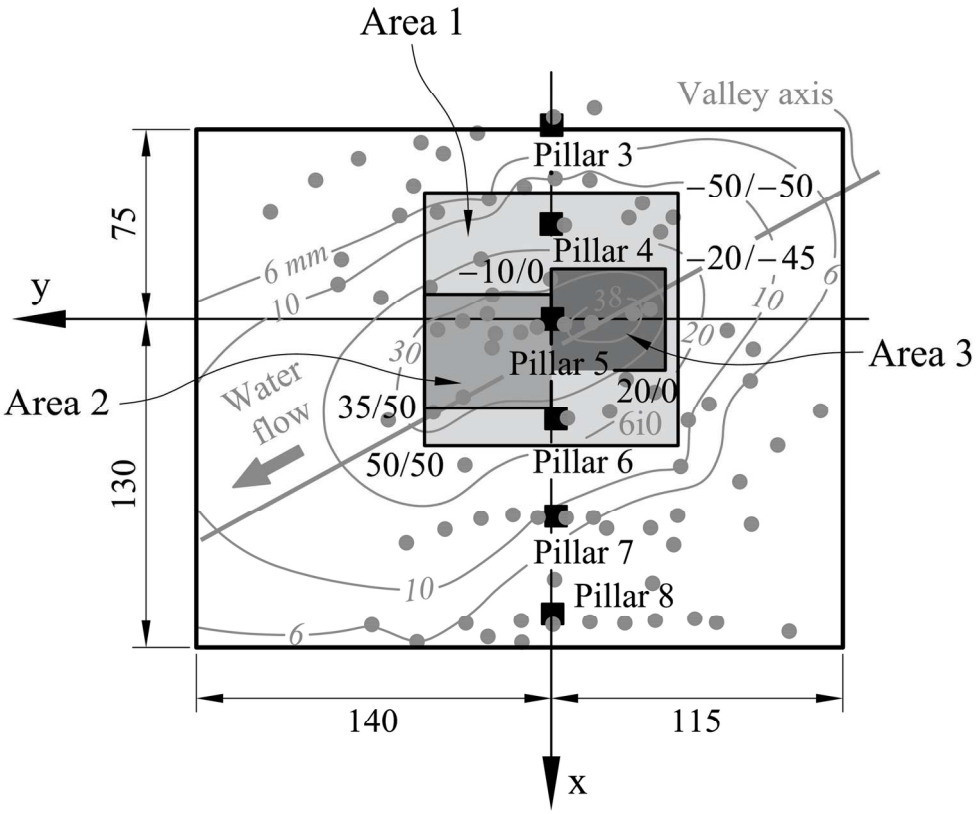

78x65mm (600 x 600 DPI)

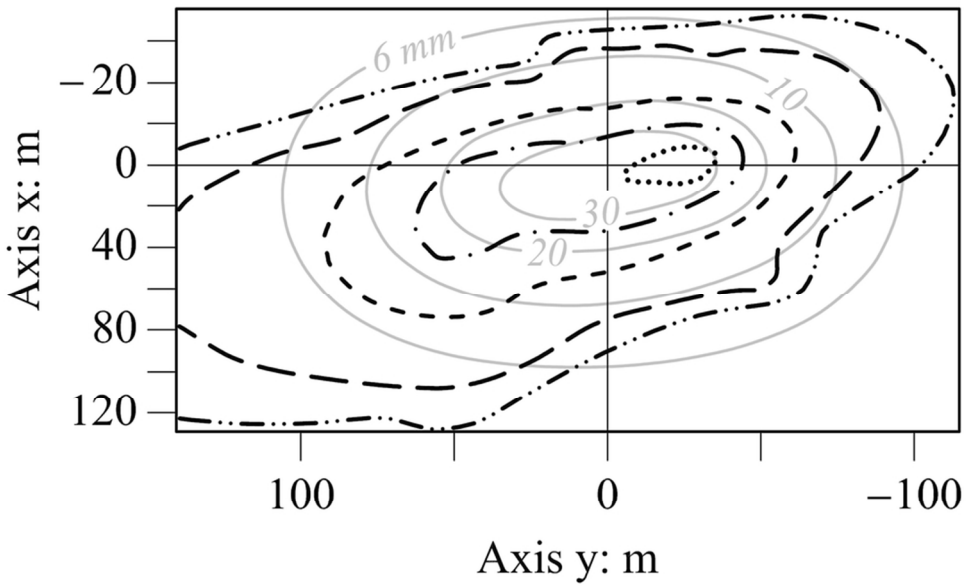

43x26mm (600 x 600 DPI)

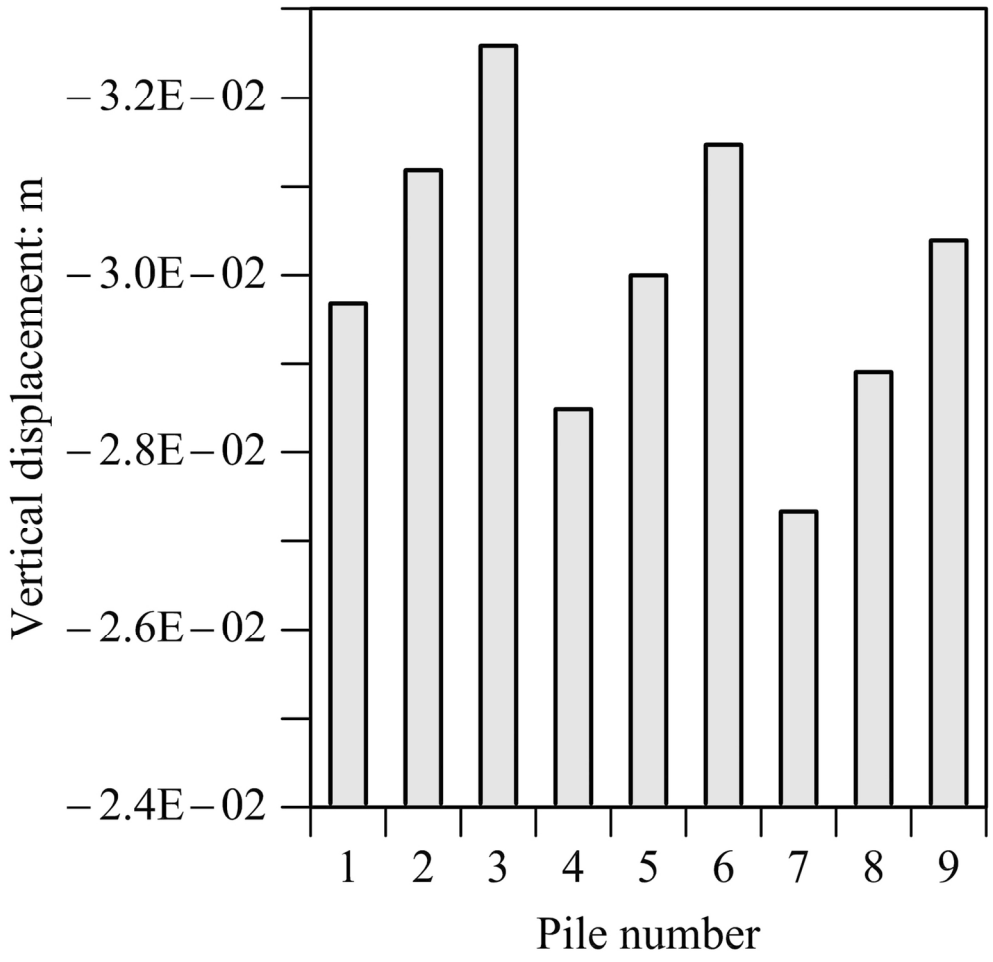

67x65mm (600 x 600 DPI)

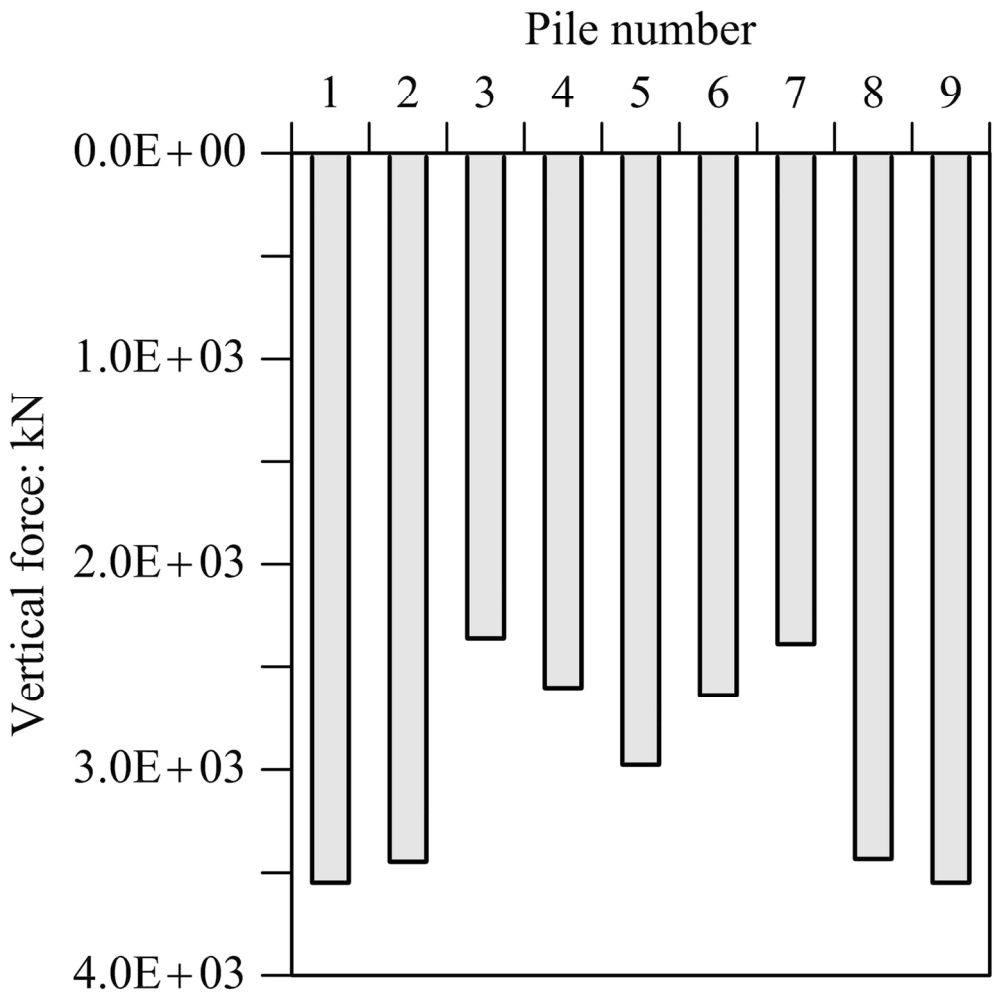

68x68mm (600 x 600 DPI)

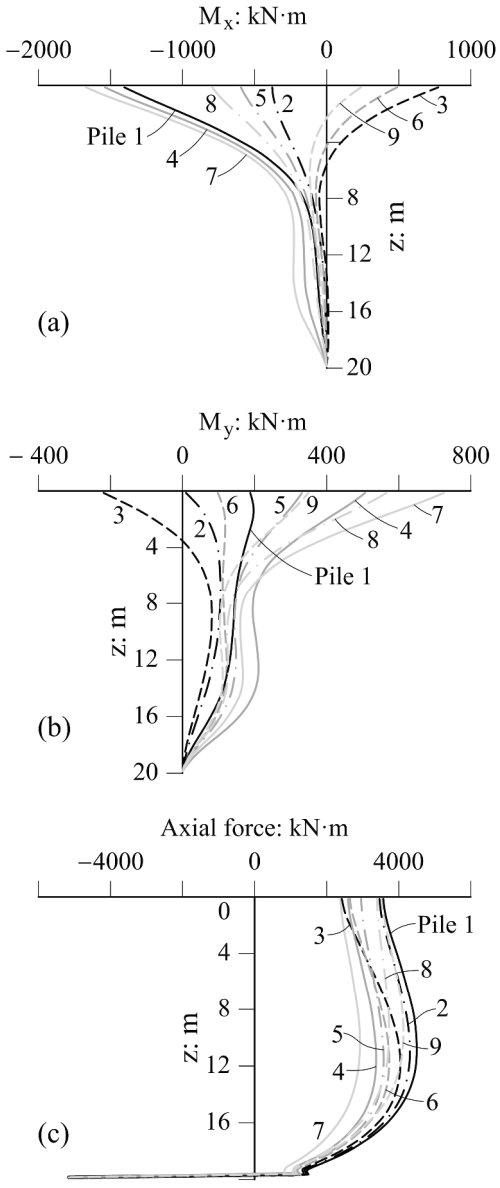

152x355mm (600 x 600 DPI)

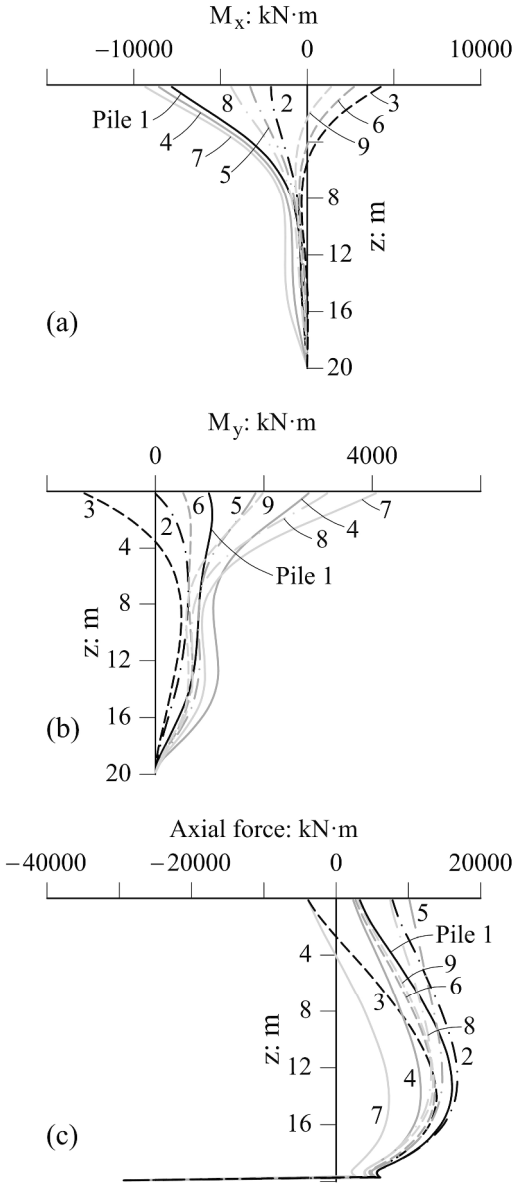

152x343mm (600 x 600 DPI)

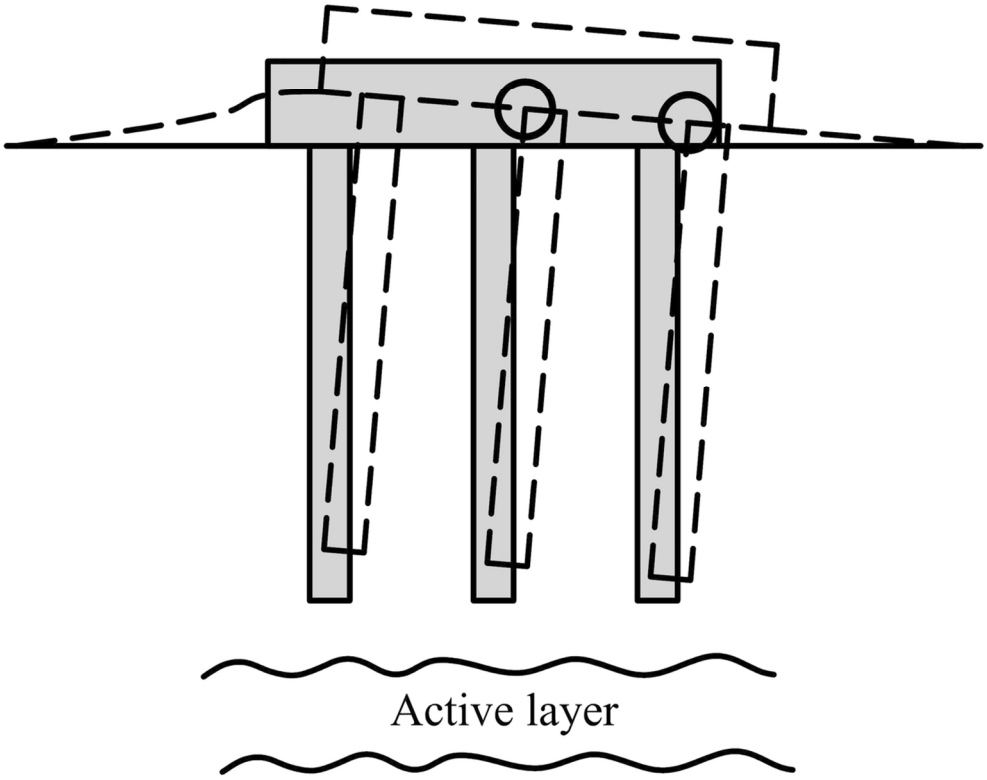

55x43mm (600 x 600 DPI)